

Polyolefin Characterization: Recent Advances in Separation Techniques

Benjamín Monrabal

Abstract New polyolefin resins, in spite of their simple chemistry, just carbon and hydrogen atoms, have become by design complex polymers with improved performance for the desired application. Besides the fundamental molar mass distribution, there are many other features that can be controlled when dealing with copolymers and new multireactor/multicatalyst resins. The average properties measured by spectroscopic techniques are not enough to define the microstructure of the new resins; it is necessary to fractionate the polymer according to certain parameters such as molar mass, branching, or stereoregularity. Separation techniques have become essential for the control and characterization of these polymers; nevertheless, full characterization is not a simple task and has demanded the development of new separation methodologies in recent years, and in many cases multiple separation techniques are required to define the microstructure. A review of the most important separation techniques with emphasis on the new technologies is given and the applications of these new polyolefin resins discussed.

Keywords Cross-fractionation chromatography · Crystallization analysis fractionation · Crystallization elution fractionation · Field flow fractionation · Gel permeation chromatography · High temperature liquid chromatography · Size-exclusion chromatography · Solvent gradient interaction chromatography · Temperature rising elution fractionation · Thermal gradient interaction chromatography

Contents

1	Introduction	205
2	Polyolefin Microstructure	206
	2.1 Polyethylene Microstructure	207
	2.2 Polypropylene Microstructure	209

B. Monrabal (✉)
Polymer Char, Valencia, Spain
e-mail: benjamin.monrabal@polymerchar.com

3	Molar Mass Distribution Characterization Techniques	211
3.1	GPC/SEC	211
3.2	Asymmetric Flow Field Flow Fractionation	217
4	Chemical Composition Distribution: Characterization Techniques	218
4.1	Crystallization-Based Techniques	219
4.2	Chromatography-Based Techniques	236
5	Bivariate Distribution: Characterization Techniques	241
6	Summary, Conclusions, and Outlook	246
	References	247

Abbreviations

AF4	Asymmetric flow field flow fractionation
aPP	Atactic polypropylene
CCD	Chemical composition distribution
CEF	Crystallization elution fractionation
CR	Crystallization rate
CRYSTAF	Crystallization analysis fractionation
DC	Dynamic crystallization
DSC	Differential scanning calorimetry
EGMBE	Ethylene glycol monobutyl ether
ELSD	Evaporative light scattering detector
EMA	Ethylene-methyl acrylate
EP	Ethylene propylene copolymer
EPDM	Ethylene-propylene diene
ESL	Ethylene sequence length
EVA	Ethylene-vinyl acetate
FC	Crystallization flow
FDSC	Fractional DSC
FE	Elution flow
FFF	Field flow fractionation
FTIR	Fourier transform infrared
HDPE	High-density polyethylene
HPLC	High-performance liquid chromatography
HR	Heating rate
HT	High temperature
IC	Interaction chromatography
ICPC	International Conference on Polyolefin Characterization
iPP	Isotactic polypropylene
IR	Infrared
LCB	Long chain branching
LDPE	Low-density polyethylene
LLDPE	Linear low-density polyethylene
LS	Light scattering
M	Molar mass

MALS	Multi-angle light scattering
MCT	Mercury cadmium telluride
MMD	Molar mass distribution
NMR	Nuclear magnetic resonance
ODCB	1,2-Dichlorobenzene
PE	Polyethylene
PP	Polypropylene
RI	Refractive index
SCB	Short chain branching
SCBD	Short-chain branching distribution
SEC	Size-exclusion chromatography
SGIC	Solvent gradient interaction chromatography
SGIC2D	Two-dimensional solvent gradient interaction chromatography
SIST	Stepwise isothermal segregation
sPP	Syndiotactic polypropylene
SSA	Successive self-nucleation annealing
STAF	Solvated thermal analysis fractionation
TCB	1,2,4-Trichlorobenzene
TGIC	Temperature gradient interactive chromatography
TREF	Temperature rising elution fractionation

1 Introduction

Polymer characterization at the time Ziegler and Natta synthesized the first linear polyolefins in the 1950s was not yet a mature science. Staudinger [1] was among the first to recognize the importance of molar mass for product properties. Molar mass was being measured by dilute solution viscosity, osmometry, ultracentrifugation or light scattering and different types of averages were obtained depending on the technique being used. It was also understood in the 1930s that synthetic polymers are polydisperse, but in the case of polyolefins it was not possible to measure the molar mass distribution until the late 1960s.

In the early stages of polyolefin development, most characterization work was focused on the catalyst itself and the understanding of polymerization mechanisms. The new polyethylenes being synthesized were being characterized by the bulk polymer properties and most effort was given to understanding the crystal structure and physical properties for a given molar mass average.

The synthesis of polypropylene brought a new scenario and major efforts at that time concentrated on controlling the stereoregularity, synthesizing the most regular isotactic polypropylene, and understanding its polymorphism; these efforts have continued for many years.

Polymer microstructure became more complex when short chain branches were inserted into the linear chains, with the addition of α -olefin comonomers with the

intention of modifying the polyethylene density. In the case of polypropylene, the addition of ethylene extended the product range to copolymers.

Characterization techniques being used in the 1950s and 1960s, such as NMR, infrared spectroscopy, X-ray diffraction, microscopy etc., could only measure the average values; this was also the case for the molar mass measurement. In some cases, there was a need to separate the amorphous and crystalline fractions by solvent extraction methods because no other means to measure the distributions were available.

We had to wait for quite some years for the development of new separation principles like gel permeation chromatography (GPC) in the late 1960s and temperature rising elution fractionation (TREF) in the late 1970s to better define the polyolefins microstructure by its distributions (molar mass and composition distributions). It took a significant time and effort to fully develop these separation techniques. Separation first means dissolution, which with the good chemical resistance of polyolefins demands a high temperature with special solvents; the second challenge is good detection, which with the lack of chemical functionality could only be done by refractive index and later on with more sensitive infrared detectors.

The development of single-site catalysts in the 1980s together with new multi-reactor processes and new comonomers opened the route for the design of new resins with improved performance for different applications. New polyolefin copolymers may have a complex microstructure and, besides molar mass and composition distribution, it is necessary to characterize the bivariate distribution (interdependence of molar mass and composition) and, on occasions, the level of long chain branching and stereoregularity.

Spectroscopic techniques have improved significantly in the last 50 years, especially in sensitivity, and they are of great value for investigating new structures or understanding the intramolecular inhomogeneity of polyolefins. However, more effort has been demanded in separation science, and the new developments to deal with the analysis of these complex structures will be the subject of this chapter.

2 Polyolefin Microstructure

Polyolefins have the simplest chemistry of all synthetic polymers, just carbon and hydrogen atoms, but can have complex microstructures. Besides the molar mass distribution, there exists a wide range of significant features in the polyolefin molecular architecture such as:

- The presence of short chain branches, by the addition of one or various comonomers, which could result in intermolecular homogeneous (single-site catalyst) or heterogeneous (multiple-site catalysts) incorporation
- The presence of long chain branches, which even in small quantities have a significant influence on rheological properties

- Stereoregularity differences in the case of polypropylene
- The recent appearance of block copolymers

Very often, with the goal of optimizing final product performance, the industrial polyolefin products are a complex combination of resins with some of the features listed above. It is not surprising that various separation techniques may be required to cover a full characterization task.

In the following sections, the microstructure features of the most important polyolefins are described.

2.1 Polyethylene Microstructure

The chemical structure of a linear polyethylene homopolymer is solely defined by the molar mass distribution (MMD) of the resin. This important distribution, together with the additives incorporated and the final morphology achieved in the processing, defines the polymer performance in a given application.

In the resin manufacturing process, and due to the difficulties in obtaining fast MMD data, homopolymer resins are controlled by a parameter related to the average molar mass (M), the melt index, and on occasions by additional rheology measurements that reflect the broadness of the distribution; however, when full characterization of a linear high-density polyethylene (HDPE) homopolymer product is required, the whole MMD must be measured.

To expand the application range of polyethylene produced with Ziegler-type [2, 3] or chromium oxide catalyst processes [4, 5], comonomers such as propylene, butene, hexene, or octene are incorporated into the linear chain and become short chain branches that reduce the crystallizability of the polymer, extending the density range from 0.96 g/mL of the HDPE homopolymer through medium density resins (0.94 g/mL) down to the linear low-density polyethylene (LLDPE) resin types (0.91 g/mL) and below to the elastomers region. The density value of a given polyethylene resin correlates to the average comonomer mole percentage incorporated; however, when dealing with multiple-site catalyst systems (Ziegler-type), the intermolecular incorporation of comonomer is not uniform and, in those cases, there is further need to know the chemical composition distribution (CCD) and the molar mass–composition interdependence.

A scheme of the extended chain molecular population and branching in an LLDPE resin is shown in Fig. 1a, where it is seen that the larger the molecule the lower chances of comonomer incorporation (lower branch content). Most interesting in LLDPE is the bimodality of the CCD, sometimes referred to as the short-chain branching distribution (SCBD), as shown in Fig. 1b, due to the population discontinuity observed between (1) the fraction of linear molecules, practically excluding the comonomer incorporation in certain catalyst sites, and (2) the remaining fractions with increasing amounts of comonomer incorporated. Catalyst sites, where the bulkier and less reactive comonomer can be incorporated,

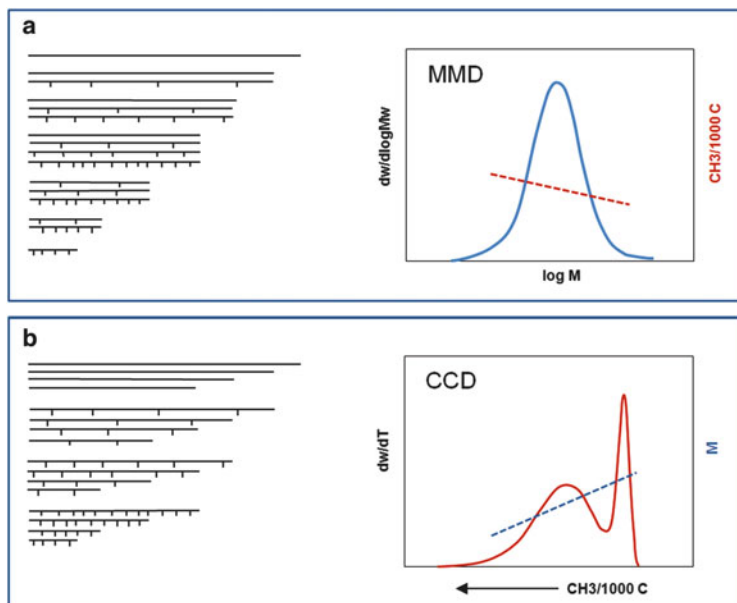


Fig. 1 (a) LLDPE molecular population organized by size and the corresponding MMD curve. (b) Molecular population organized by composition (branching) and the corresponding CCD curve. M molar mass

result in higher chances of thermal termination and thus lower molar mass, as shown by the crossing lines in the MMD and CCD plots of Fig. 1 which provide a two-dimensional (2D) view of the molar mass–composition interdependence.

The development in 1980 of single-site metallocene catalysts by Kaminsky [6, 7] resulted in a better-defined polyethylene microstructure, with uniform intermolecular comonomer incorporation and narrow MMD; this development opened new applications by copolymerizing new comonomers, extending the polyethylene range to the elastomers region, and providing a means to resin design through multiple reactor-catalyst technologies. A good example is shown schematically in Fig. 2, where a high molar mass polymer of low density produced with a single-site catalyst is combined with a Ziegler-type resin of lower molar mass. The design possibilities for optimizing the polymer performance with this particular combination by changing the comonomer incorporation and thermal termination in each reactor are also illustrated in Fig. 2.

The development of improved performance HDPE pipe resins by the so-called inverse process, incorporating the comonomer in the high molar mass (not possible with Ziegler-type catalysts in a single reactor) is also an excellent example of design through dual reactor and multiple catalyst technologies.

Another family of low density polyethylenes (LDPE) can be obtained by high-pressure free radical polymerization, resulting in complex microstructures where side chain branches (mainly ethyl and butyl) are obtained through chain transfer reactions without the need of comonomer incorporation. The presence of long

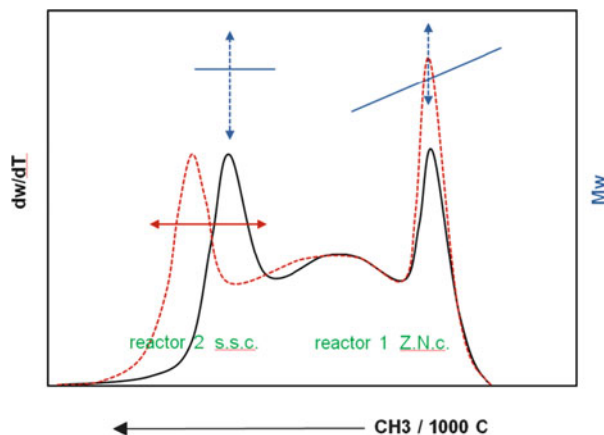


Fig. 2 CCD of a multireactor resin. Combination of a Ziegler-type resin (*reactor 1*) with a single-site resin (*reactor 2*) and possible combinations of comonomer incorporation and molar mass changes

chain branches (LCB) and the possibility of incorporating polar comonomers like vinyl acetate are features of the free radical polymerization process. The measurement of the MMD and the LCB distribution are the most important characterization tasks in these complex LDPE resins.

2.2 Polypropylene Microstructure

Polypropylene homopolymers besides the measurement of the MMD need further characterization to fully describe their microstructure due to the existence of the tertiary carbon in the propylene molecule.

When the insertion of propylene molecules in the growing chain is such that all methyl branches are on the same hand, the regularity of the chain allows it to crystallize; this is the isotactic polypropylene (iPP), synthesized by Natta [8, 9] and the most commercial type obtained by the Ziegler–Natta stereoregular polymerization process. When the monomer insertion is consistently in the opposite hand to previous monomer insertion, the polymer obtained is syndiotactic polypropylene (sPP), which achieves lower crystallinity and today has less commercial interest. The random stereo incorporation of monomer units results in an amorphous resin, atactic polypropylene (aPP).

Besides the three types discussed above and represented schematically in Fig. 3a, there may happen undesired stereo errors in the growing chain which will reduce the tacticity or, regio errors when instead of inserting the new monomer head to tail, it does head to head or tail to tail, disrupting the methyl sequence. These features have been extensively investigated by NMR and in all cases result in modification of the stereoregularity and crystallinity.

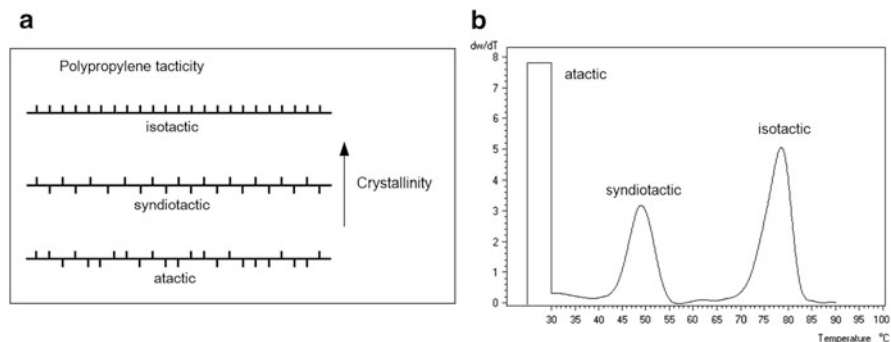


Fig. 3 (a) Various tacticity configurations in PP. (b) Crystallization temperatures in solution (CRYSTAF) of the three tacticity forms of PP

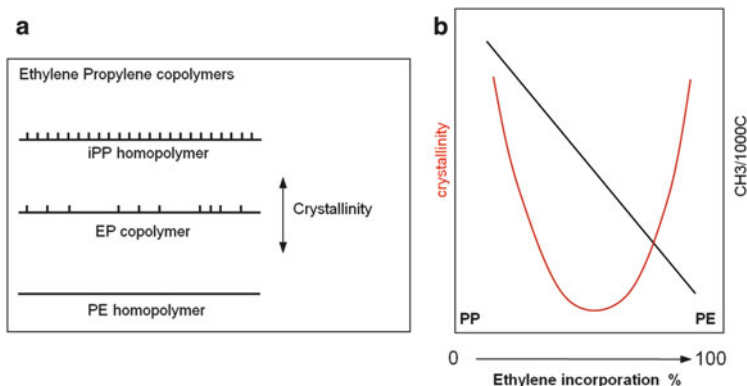


Fig. 4 (a) Disruption of the methylene sequence in iPP by randomly incorporating ethylene to produce an EP copolymer. (b) Crystallinity and branching of PE, PP, and the range of EP copolymers

The analysis of the distribution of intermolecular tacticity in a blend of the three PP types discussed above is shown in the crystallization analysis of Fig. 3b. Any additional disruption of the stereoregularity of iPP or sPP will result in lower crystallinity and peaks will be shifted towards lower crystallization temperatures.

In the case of polypropylene copolymers, typically ethylene propylene (EP) copolymers, the insertion of ethylene into the growing PP chain will result (for the same reasons as discussed above) in disruption of the methyl sequence and thus reduce the crystallizability, as shown in Fig. 4a. In terms of crystallinity, the addition of ethylene in EP copolymers result in a u-shape curve, as shown in Fig. 4b where both homopolymers have a higher crystallinity than the intermediate EP copolymers.

When analyzing the microstructure of polypropylene homo- and copolymer resins by crystallization techniques, all those aspects need to be considered in the interpretation of the crystallization/dissolution curves (often referred to as CCD, as in the case of PE resins). The analysis of polypropylene and polyethylene

blends is further complicated by the large differences in undercooling of both resins, as will be discussed in sect. 4.1.3.

3 Molar Mass Distribution Characterization Techniques

The molar mass distribution (MMD) is the most fundamental structural parameter for all homopolymers and, together with the CCD and their interdependence (bivariate distribution), defines the microstructure of most polyolefin copolymers. Until the late 1960s, only molar mass averages could be obtained by light scattering, osmometry or viscosity measurements. It requires a separation process to measure the full MMD, and this only became available with the development of gel permeation chromatography (GPC) by Moore in 1964 [10], which represented a significant contribution in the polymer chemistry field. Today most MMD data for synthetic polymers are obtained by this chromatographic technique.

In recent years, field flow fractionation (FFF) [11], which has been used with success in biological macromolecule separation, has become available for the measurement of the MMD of very high molar mass resins.

3.1 GPC/SEC

Gel permeation chromatography (GPC) is also known as size-exclusion chromatography (SEC) and both names are used today in the literature. The GPC technique has been extensively used in the last 50 years and has contributed to the development of polyolefin catalysts, processes, and the improvement of resin performance. There exist good references that deal with the fundamentals of the technique [12, 13], calibration procedures [14–16], and the analysis of LCB [17–23], which still demands significant attention.

In this review, we will focus on the new and most recent technological developments in automation, infrared detection, and its applications in polyolefin analysis.

GPC instrumentation for high temperature analysis, being a niche market, has remained unchanged for a long time. In recent years, new instrumentation has been introduced with significant engineering advances [24] like modular design to facilitate maintenance tasks, larger volume vials to reduce sample non-homogeneity, automated sample preparation (filtration included), and having a separate column oven compartment to prevent column damage during maintenance tasks.

A large amount of attention has been put into minimizing polymer degradation during the sample preparation because of the high temperature and large time required for polyolefins dissolution (including the waiting time for injection in autosamplers) and to reduce the potential shear degradation during stirring and filtration. The dual temperature zone autosamplers developed in the 1990s and the incorporation of antioxidant in the dissolution process provided an improvement, but not enough for the very labile polypropylene resins that may suffer chain

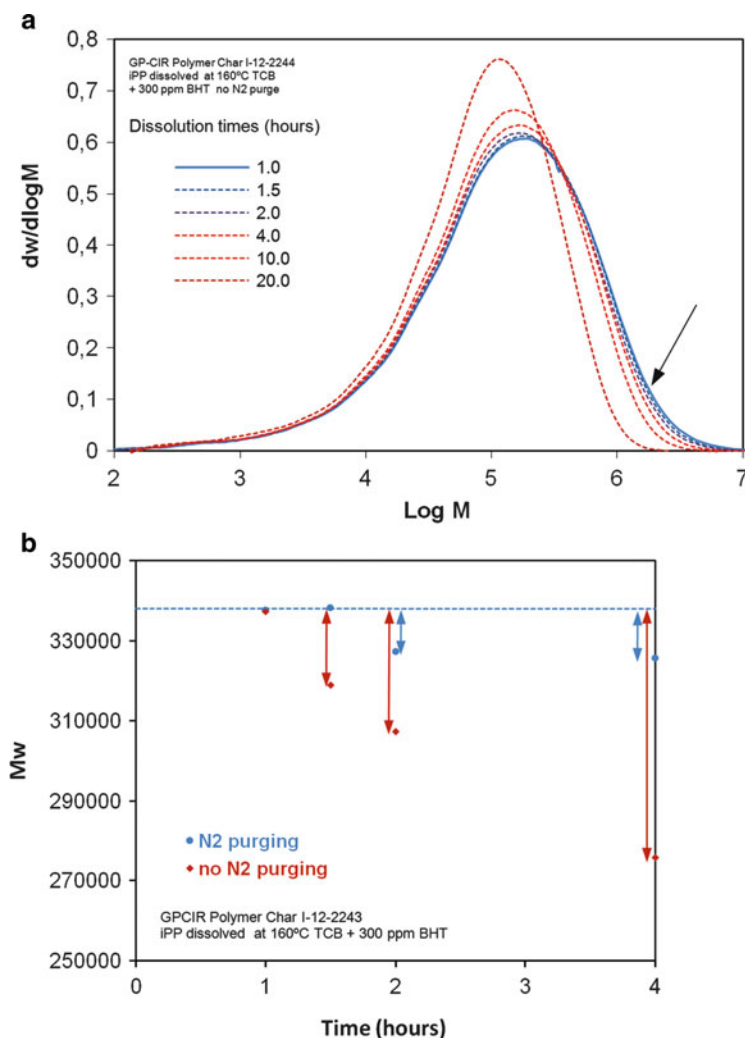


Fig. 5 Polypropylene degradation during dissolution at high temperature. (a) Shift of MMD and (b) weight-average molecular mass (M_w) versus dissolution time in TCB with 300 ppm BHT, with and without nitrogen purge

scission during dissolution even at shorter times than expected [25]. New approaches have been presented recently to prevent polymer degradation, like using a better solvent (decaline) for the sample dissolution step at lower temperatures [26] or by new autosamplers that allow for nitrogen purging of the vial and precise dissolution time of each sample [27], eliminating the waiting time for injection of the current systems. The importance of nitrogen purging and the influence of dissolution time in degradation of the various polyolefins have been presented recently [28] and can be seen in Fig. 5 for polypropylene.

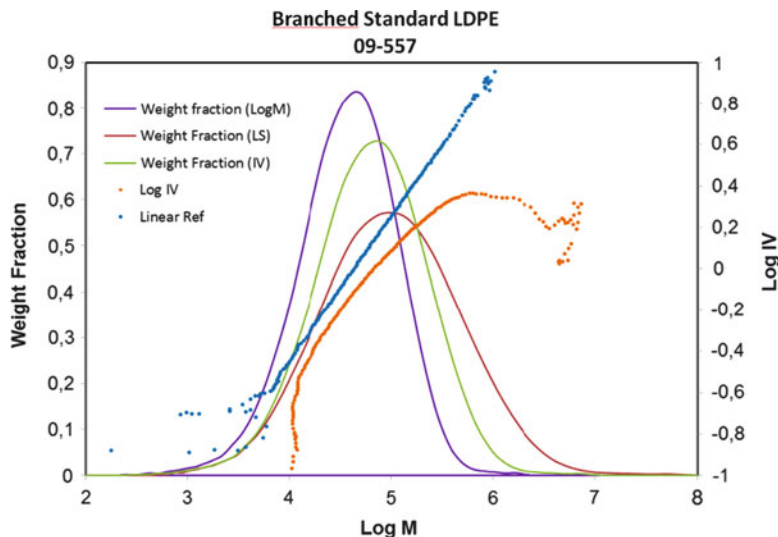


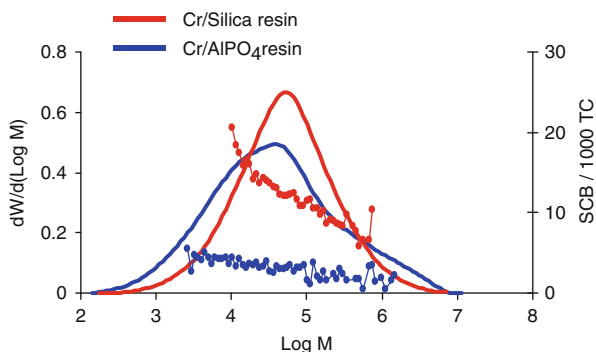
Fig. 6 Triple detector GPC analysis of a LDPE resin; only one light scattering (LS) angle is shown, IV intrinsic viscosity

For detection, modern multiangle light scattering (LS) detectors have appeared on the market for comprehensive molar mass and size measurements, e.g., from Wyatt Technology (Santa Barbara, CA) [29] as well as single small-angle compact LS system integrated into the detection block (e.g., from Malvern Instruments, Worcestershire, UK) [30]. The use of triple detector GPC (GPC-3D) remains a very active field. An example of GPC-3D analysis is shown in Fig. 6, using concentration, viscosity, and light scattering signals to measure the LCB in a LDPE resin [17–23].

Refractive index detectors remained for many years the most popular concentration detectors in GPC. In the case of polyolefin analysis, however, infrared (IR) detection was shown quite early to be more appropriate [31, 32]. These detectors are filter-based pyroelectric sensing elements (at specific wavelengths) with a heated flow-through cell attached at the exit of the GPC columns; they were used by some polyolefin laboratories in the 1970s although IR detector technology was not yet fully developed, and it did not become popular until the early 2000s [33]. The chlorinated solvents used in the GPC analysis of polyolefins [1,2-dichlorobenzene (DCB), 1,2,4-trichlorobenzene (TCB), and perchloroethylene] do not contain aliphatic C–H bonds and, thus, allow for the analysis of polymer concentration by measuring absorption at around 3.5 μm (aliphatic C–H stretching band).

With the development of FTIR, infrared detection attached to GPC with a flow-through cell became interesting in the 1990s for obtaining the comonomer incorporation (short chain branches) in polyolefin copolymers by measuring, besides concentration, the number of methyl groups per 1,000 carbon atoms ($\text{CH}_3/1000\text{C}$) along the molar mass [34–36]. The measurement of very low levels

Fig. 7 Analysis of a HDPE pipe resin by GPC FTIR. *SCB* short chain branches, *TC* total number of carbon atoms [37]



of branches was shown to be possible by DesLauriers et al. [37, 38] using nitrogen-cooled MCT detectors (mercury cadmium telluride sensing element) in combination with a chemometric approach, as shown in Fig. 7. This technique has been further optimized by Piel [39] and Albrecht [40].

In the late 1990s, new and compact optoelectronic IR detectors [33] were developed using interference filters at selective wavelengths. They soon became popular for polyolefin GPC analysis because of their sensitivity, short stabilization time, and low temperature dependence. The IR detector results in a cleaner detection of sample components in the low molar mass tail of the GPC elution curve as compared to the refractive index, which often shows solvent impurities and negative peaks in the very low molar mass region. IR detectors used with a flow-through cell are, however, restricted to applications where the solvent is transparent enough in the spectrum region of interest. Typically, two interference filters are used, one measuring the overall absorption of the C–H region and a second centered at the absorption of the C–H from the methyl groups. The analysis of a polypropylene and polyethylene blend is shown in Fig. 8a, with the two signals obtained simultaneously. The ratio of the two signals is directly proportional to the presence of methyl groups, and it can be easily calibrated as the percentage of ethylene incorporated in EP copolymers. The analysis of three EP resins having similar MMD but completely different ethylene incorporation is shown in Fig. 8b.

The simultaneous analysis of concentration and composition in GPC measurements is of significant interest for today's complex polyolefin copolymers. The same IR detector can be used to analyze ethylene-vinyl acetate (EVA) or other functional polyolefin copolymers (with a carbonyl group) as a function of molar mass. All that is needed is to replace the “methyl” interference filter by a “carbonyl” region filter. An example of a maleic anhydride-modified PE is shown in Fig. 9, with an IR interference filter measuring at $1,740\text{ cm}^{-1}$.

More recently a new filter-type IR detector has been developed [41] with a highly sensitive MCT thermoelectrically cooled sensing element. It has similar response in the C–H region to that of FTIR detectors but it does not require nitrogen cooling. The integration of this detector, in a thermostated compartment, into a GPC system has resulted in an improvement of sensitivity of around ten times

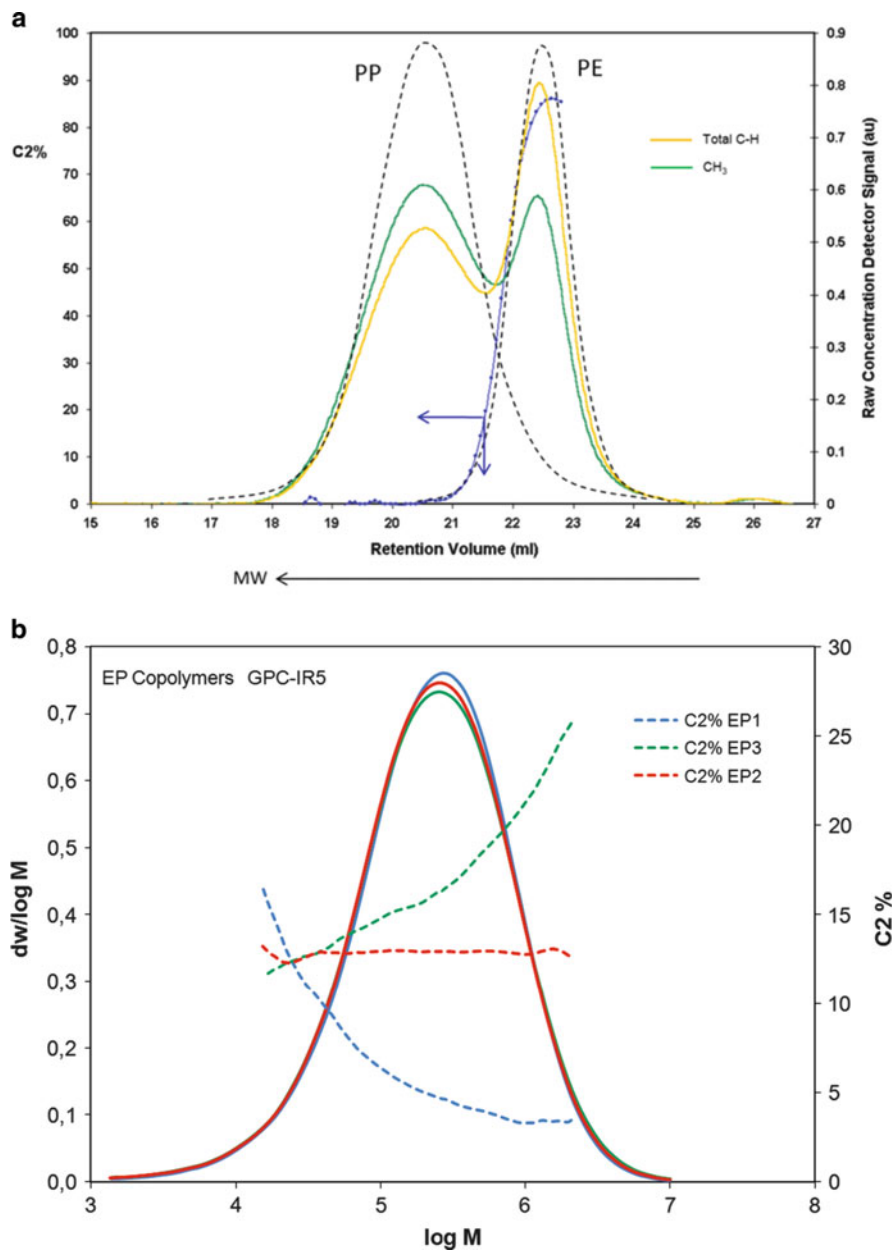


Fig. 8 (a) Analysis of a PE resin of low molar mass and a PP resin of high molar mass in a GPC-IR instrument (*dashed lines*) and a 50/50 blend of both resins, showing the total C–H concentration (*gray solid line*) and the C–H centered at CH₃ absorption (*solid line*). The *dotted solid line* corresponds to the ratio of methyls to total concentration, calibrated in percentage ethylene incorporation (C2%). (b) Analysis by GPC-IR of three different EP copolymers (EP1, EP2, and EP3) having similar MMD but completely different ethylene incorporation along the molar mass (*M*)

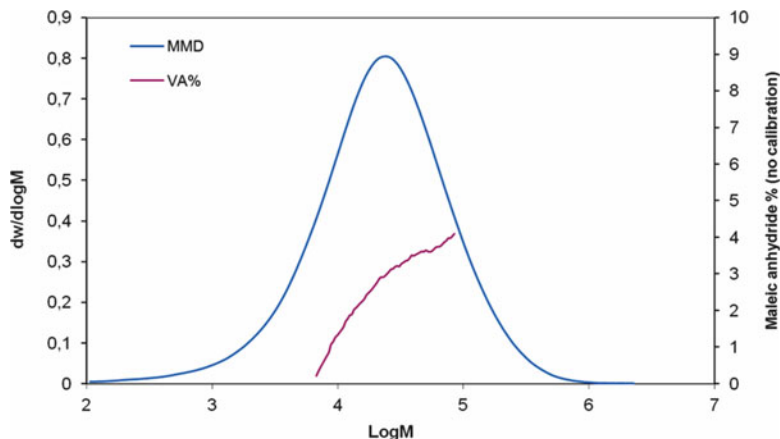


Fig. 9 Analysis of a maleic anhydride-modified PE by GPC-IR to characterize the interdependence of composition and molar mass. Calibration was with vinyl acetate (VA) standards

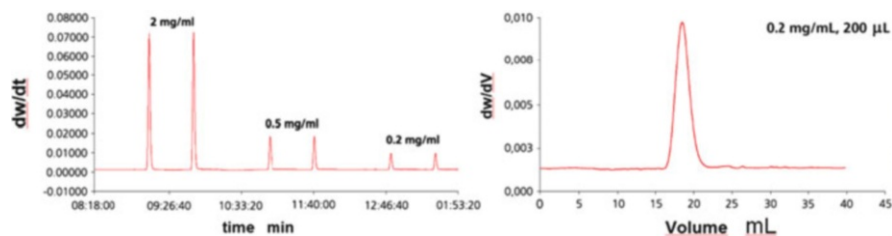


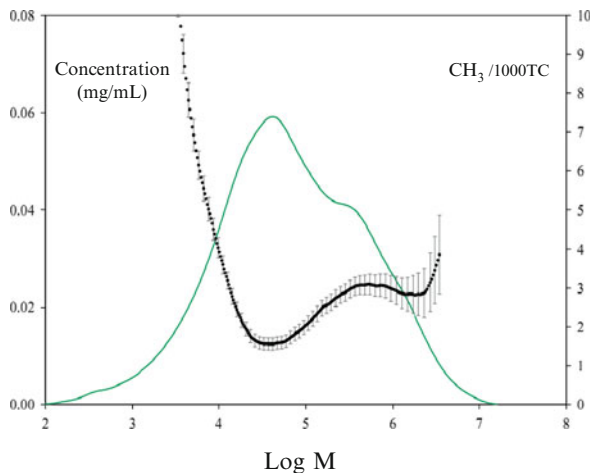
Fig. 10 (a) Duplicate analysis of an ethylene octene copolymer at different concentrations by GPC-IR using an integrated thermoelectrically cooled MCT detector. (b) Expanded view of the GPC-IR analysis at a very low concentration of 0.2 mg/L

over existing IR detectors [42], as shown in Fig. 10 by the good signal-to-noise ratio and baseline stability obtained after injecting a PE sample that was ten times more dilute than the concentration used under standard GPC conditions.

The sensitivity improvement with this new detector is obtained for both concentration and composition signals, and thus it is being used with success for the difficult analysis of HDPE pipe resins that have low comonomer incorporation [43]. The calibration and error analysis in this difficult application have been studied recently by Ortín et al. [44] and an example of a pipe resin analysis is shown in Fig. 11.

In previous sections we have referred to the combination of IR and GPC, with online detection using a flow-through cell, and the IR system being an integrated filter-type detector or an external FTIR spectrometer. There exists the option to deposit the fractions coming from the GPC column onto a germanium disk while evaporating the solvent, and later measuring the full FTIR spectrum of the various polymer spots in the disk to obtain similar information on composition and molar mass interdependence [45–47] as in previous sections. This approach has been

Fig. 11 GPC-IR of a pipe resin. Branching and error analysis



recently improved by using microscopic technology on the IR beam [48, 49]. In those cases, the information obtained from the IR spectra (without the presence of solvent) is superior and very powerful for the qualitative identification of unknown copolymers and additives, although it demands more time for analysis and method optimization. On the other hand, GPC-IR with a flow-through cell is being used for analysis of copolymers of known chemistry and provides better quantitation in a shorter time and with less manpower requirements.

The combination of proton NMR and GPC was shown to be possible by Hiller et al. [50], who built a setup to analyze a blend of PE and poly(methyl methacrylate) (PMMA).

3.2 Asymmetric Flow Field Flow Fractionation

Field flow fractionation (FFF) developed by Giddings [11] in 1966 is a non-column separation technique that has been shown to be of great value for the separation of biological macromolecules. The separation takes place by flowing the solution in a flat channel with no stationary phase, and when being used in the asymmetric flow field flow fractionation (AF4) mode [51], a cross-flow perpendicular to the solvent flow is added, as shown in Fig. 12, which leaves through a semipermeable membrane. A field force against the membrane is formed, with polymer molecules being driven to different heights in the channel over the membrane depending on their diffusion coefficients. The smaller molecules, diffusing faster, are positioned far from the membrane and are flushed at a higher flow velocity than the larger molecules that stay closer to the membrane, where the flow is lower due to the channel parabolic flow profile.

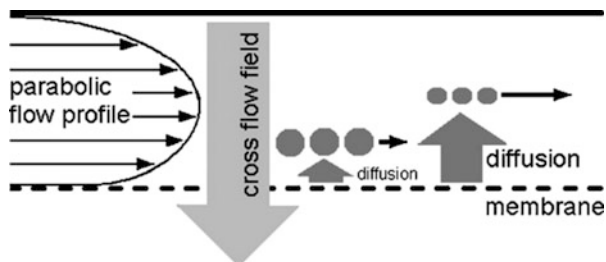


Fig. 12 Separation mechanism of asymmetric flow field flow fractionation (AF4). Small molecules diffuse faster and away from the wall, eluting at higher flow velocity than larger molecules [53]

The limitations of GPC for separation of large macromolecules, i.e., the unavailability of proper columns and the potential shear degradation of high macromolecules in a frit or column packing, are avoided in AF4 by the separation at the empty channel.

The application of high-temperature AF4 to polyolefins was first investigated by Mes et al. [52], who showed better separation with AF4 in very high molar mass LDPE and HDPE than with GPC. This work was continued by Otte et al. [53, 54], who optimized the operation conditions. The major drawback of the technique at this time was the limit for low molar mass materials (50,000 g/mol) because of the difficulties in producing membranes of low-enough pore size.

4 Chemical Composition Distribution: Characterization Techniques

In the previous section, we have seen that the combination of GPC with IR detection provides a measurement of the comonomer incorporation (composition) versus molar mass; however, this does not tell us about the intermolecular distribution of branches (or any other polar comonomer incorporated) into the linear chains, which we refer as the CCD. This also needs to be measured independently in most polyethylene copolymers.

In the case of polypropylene homo and copolymer resins, besides the CCD, which is related to the ethylene incorporation, there is an additional feature, the tacticity, which very often is measured combined with the CCD. In all cases, low tacticity or the incorporation of comonomers result in reduced crystallinity; therefore, it is understandable that most popular techniques for the measurement of the CCD are based on the crystallizability of the polymer.

Calorimetric methods have been used to obtain qualitative data or parameters that could correlate with the CCD [55–57]. It should be clear, however, that differential scanning calorimetry (DSC), although very powerful in other areas, does not provide the ideal environment for crystallization, does not result in

quantitative mass measurements (measuring the heat flow instead of concentration), and has less sensitivity for less crystalline materials; nevertheless, DSC methods have been available and used with certain success before solution crystallization techniques were developed. A short review of the calorimetric techniques used in this application will be presented in Sect. 4.1.1.

The most comprehensive analytical methods being used today to measure the CCD are based on a separation process according to crystallizability. They are performed in solution (higher chain mobility), which result in improved resolution and less co-crystallization effects. In following sections, three separation techniques to measure the CCD based on crystallizability will be described (see Sects. 4.1.2, 4.1.3, and 4.1.4):

- Temperature rising elution fractionation (TREF)
- Crystallization analysis fractionation (CRYSTAF)
- Crystallization elution fractionation (CEF)

In the last 5 years, a new chromatographic approach has been developed to separate polyethylene copolymers by adsorption on a carbon-based column according to composition, with a significant interest in the characterization of less crystalline materials (elastomers). This high temperature liquid chromatography separation process can be performed by solvent gradient or through thermal gradient and has evolved into the following two techniques:

- Solvent gradient interaction chromatography (SGIC)
- Thermal gradient interaction chromatography (TGIC)

which will also be described in coming sections (Sects. 4.2.1 and 4.2.2).

4.1 Crystallization-Based Techniques

The principles of polymer fractionation by solubility or crystallization in solution have been extensively reviewed on the basis of Flory–Huggins statistical thermodynamic treatment [58, 59], which accounts for melting point depression by the presence of solvents. For random copolymers the classical Flory equation [60] applies:

$$\frac{1}{T_m} - \frac{1}{T_m^0} = -\frac{R}{\Delta H_u} \cdot \ln(p), \quad (1)$$

where p is the molar fraction of the crystallizing unit. Equation (1) can be reduced to:

$$T_m \cong T_m^0 - \frac{R(T_m^0)^2}{\Delta H_u} \cdot N_2, \quad (2)$$

where N_2 is the molar fraction of the comonomer incorporated. The presence of non-crystallizing comonomer units, diluents, and polymer end-groups all have an equivalent effect on melting point depression when the concentration of each is low and they do not enter into the crystal lattice. From (2), a linear dependence of melting or crystallization temperature T_m with the amount of comonomer incorporated N_2 should be obtained.

In experimental practice, a straight-line correlation between temperature and comonomer composition has been obtained by various authors with TREF [61, 62], DSC [63], and CRYSTAF [64]. These correlations are practically independent of molar mass.

The importance of co-crystallization in polyethylene has been widely investigated by Alamo et al. [65]. Co-crystallization will always be present to a certain degree when crystallizing a heterogenous resin, and especially when carrying it in the melt [66] or in concentrated solutions. At the low concentrations used in modern separation techniques like TREF, CRYSTAF, or CEF, the co-crystallization effects [64, 67, 68], although present, can be in most cases neglected if low-enough crystallization rates are being used, and the separation considered to occur on the basis of comonomer incorporated (assuming intramolecular uniformity). Crystallization will happen according to the ethylene sequence length (ESL) and, if broad distributions of ESL are present, separation by crystallizability will take place according to the largest ESL, complicating the microstructure characterization. Preparative fractionation and subsequent analysis by NMR will provide more light on the analysis of branching clusters in resins with non-uniform intramolecular incorporation of branching.

4.1.1 Calorimetric Methods

Differential scanning calorimetry (DSC) has been used to obtain semi-quantitative data of the CCD. The most significant methods, or parameters, using DSC are: stepwise isothermal segregation, SIST [55]; solvated thermal analysis fractionation, STAF [69]; DSC index [57]; step crystallization [56]; successive self-nucleation/annealing, SSA [70, 71]; and fractional DSC, FDSC [72]. The advantage of calorimetric methods is the technique simplicity, not requiring the polymer dissolution. Calorimetric methods, however, suffer from low resolution and high co-crystallization due to the low mobility of polymer chains in the melt. Calorimetric methods provide a response in heat flow (not mass) and therefore overemphasize the CCD curve as moving towards the more crystalline fractions. In spite of possible correction for the nonlinear detector response, the signal-to-noise ratio will decrease with lower crystallinity of the material.

A review on thermal fractionation methods has been presented by Müller and Arnal [73], who recall that DSC methods are sensitive to both intra- and intermolecular defects whereas solution crystallization methods, where separation takes place according to crystallizability, are more sensitive to inter- than intramolecular heterogeneity.

When dealing with block copolymers, the calorimetric methods may provide some additional information not accessible by TREF, where the dominating separation mechanism is according to the most crystalline part of the block copolymer.

4.1.2 Temperature Rising Elution Fractionation

The most comprehensive analytical approach to characterizing the CCD in recent years has been TREF, implemented in the polyolefin characterization world by Wild et al. in the late 1970s [74, 75], which led to an understanding of the LLDPE structure in relation to the multiple sites in Ziegler-type catalyst.

The initial dissolution fractionation of polyethylene according to composition by increasing temperature was first described by Desreux and Spiegels [76] in 1950 using an extraction technique with a single solvent at increasing temperatures. This was used with success by Hawkins and Smith [77] and Shirayama et al. [78], who first named the technique temperature rising elution fractionation, but it was the work of Wild et al. [74, 75] in the late 1970s with the development of analytical TREF that established the technique as a standard in the polyolefin industry. Various reviews on TREF have been published by Wild [79], Glöckner [68], Monrabal [80], Fonseca and Harrison [81], Soares and Hamielec [82, 83], and recently by Monrabal in a comprehensive review chapter in the *Encyclopedia of Analytical Chemistry* [84].

The TREF analytical process resembles a liquid chromatography separation with a column, an eluent, and a detector or collecting device depending on whether an analytical or preparative approach is intended. TREF needs to be performed at the high temperatures (up to 160°C) demanded by the polyolefin dissolution step. In TREF, the separation requires two temperature cycles (crystallization and dissolution) as shown schematically in Fig. 13. Once the polymer sample is dissolved in a proper solvent at high temperature, the solution is introduced into a column containing a non-active support; this is followed by a crystallization step at a slow cooling rate during which polymer fractionation will occur, as the temperature drops, by deposition (crystallization) of layers of decreasing crystallinity or increasing branch content on the column support particles; fractionation takes place within this cycle that is usually carried out at a low crystallization rate.

At this stage, the polymer is already segregated into crystal aggregates of different composition on the inert support particles inside the column although all of them are still mixed together (there is not yet a physical separation of fractions). The TREF technique still requires a second temperature cycle to quantify or collect those fractions of different crystallinity. This is achieved by washing the column with new solvent while the temperature is being increased. The eluent dissolves fractions of increasing crystallinity, or decreasing branch content, as temperature rises. These fractions are monitored with an IR detector (analytical TREF) to generate the CCD curve, or collected (preparative TREF) to perform further analysis. The name temperature rising elution fractionation comes from this second temperature cycle.

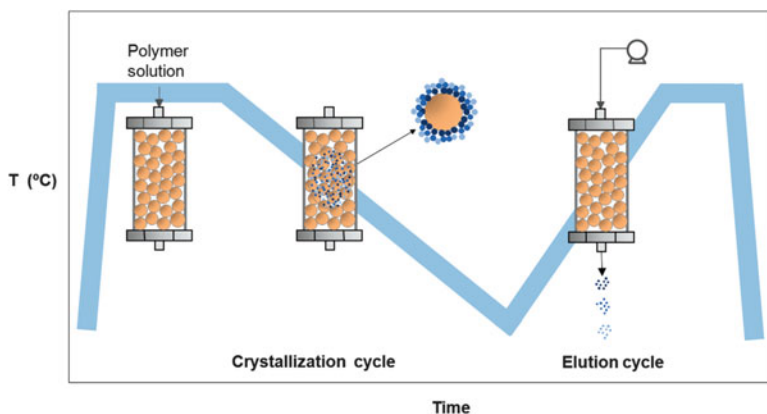


Fig. 13 The TREF process

A TREF apparatus is essentially an HPLC system with a high temperature oven to perform the crystallization and elution steps. TREF did not become commercially available until the early 1990s and most TREF users developed their own instrumentation, in most cases using an IR detector measuring the absorbance at around $3.5\ \mu\text{m}$ (C–H stretching band).

As with GPC, automation of a TREF apparatus is important to minimize solvent handling and to reduce manpower involvement and there have been various approaches in the past. Hazlitt et al. [85] reported an automated TREF apparatus with four columns in independent ovens. More recently, a fully automated TREF apparatus was introduced commercially [86] in which a significant effort was made on the sample preparation step. Up to five samples can be loaded at a time and the whole process is automated from sample dissolution to column loading and temperature rising elution; once the analysis of the first sample has been completed, the equipment continues with the dissolution and analysis of the other samples. A schematic diagram is shown in Fig. 14.

The demand for faster TREF analysis prompted the use of autosamplers, which can replace the dissolution vessels shown in Fig. 14 and avoid keeping samples at high temperature for longer times than required [87]. Yau and Gillespie [88] built a combined GPC and TREF apparatus on an existing GPC instrument that could share autosampler, pump, and detectors for both techniques.

TREF columns are typically 10–15 cm long and with an internal diameter of 3–9 mm. The columns are filled with an inert support such as glass beads, diatomaceous earth (Chromosorb), or stainless steel shots of 100–200 μm particle size.

The solvents used in analytical TREF are limited to chlorinated solvents, mainly *ortho*-dichlorobenzene and 1,2,4 tri-chlorobenzene (perchloroethylene and α -chloronaphtalene have also been used), which can dissolve the polyolefins at high temperature and are transparent enough in the IR region of measurement. These solvents are the same as used in GPC/SEC analysis of polyolefins and are also appropriate for detection by refractive index, although this detector has not

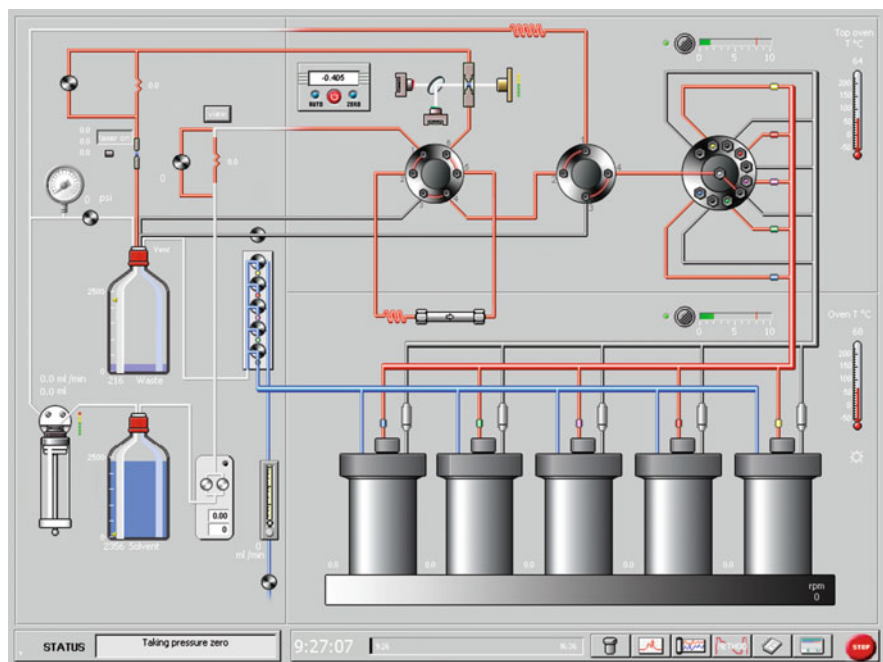


Fig. 14 TREF instrument operation diagram. In-line viscometer and light scattering detectors

been very popular in TREF due to its strong sensitivity to temperature changes in this non-isothermal process. Today, the solvent most used is *ortho*-dichlorobenzene because of its low freezing point (-17°C), which allows crystallization to sub-ambient conditions, thus extending the crystallization range for the analysis of less crystalline resins. The solvent does not influence the separation mechanism in TREF analysis but elution temperatures will be shifted depending on the solvent power, as discussed by Glöckner [68]. Monrabal et al. [89] have shown the possibility to extend the TREF analysis to less crystalline polymers by the use of more polar solvents.

Solution concentrations of 0.5% are usually prepared in vials or dissolution vessels and injection of 1–5 mg of polymer are loaded onto the column in analytical TREF. The more sensitive detectors should be used to allow for the lowest concentration possible in order to reduce co-crystallization and entrapment effects. Polyolefin homopolymers, which elute in a narrow temperature range, may often result in column plugging, especially if they have large molar mass; in those cases, a lower concentration of sample should be used for injections.

In TREF analysis, besides the mass of polymer injected into the column, the dissolution and flow rates will contribute to the detector signal response. The mass of polymer being dissolved per unit time is proportional to the heating rate, thus the concentration reaching the detector can be expressed by (3), where HR is the heating rate, F the flow rate and k is a function of the polymer microstructure and mass injected:

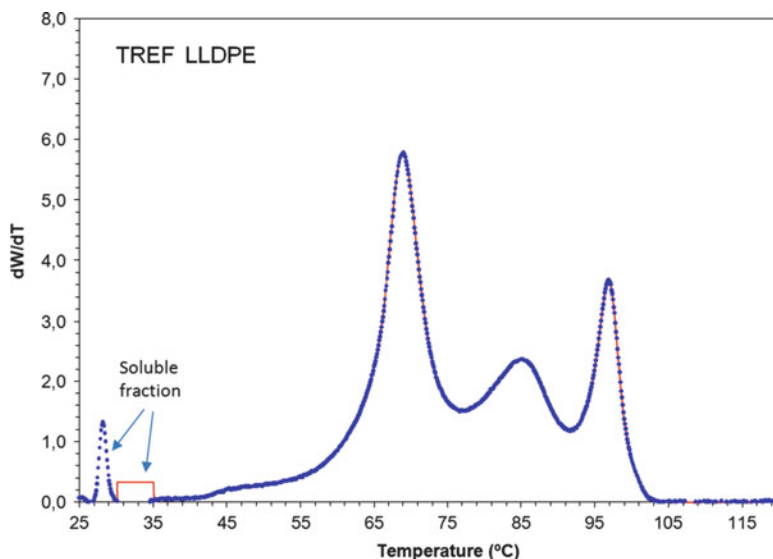


Fig. 15 TREF analysis of a LLDPE resin. Soluble fraction as eluted (*peak*) or after calculation (*rectangle*)

$$c = k \cdot HR/F. \quad (3)$$

For the same amount of sample injection, keeping the HR/F ratio constant will maintain the same detector response.

The crystallization process is the most important step in the TREF analysis; it is in this process where fractions are segregated according to their crystallizability and it is preferably used at the lowest cooling rate to minimize co-crystallization effects. The lowest crystallization rate (CR) will also result in most stable crystal aggregates and will prevent unwanted re-organization during the following melting process. Typically CR of 0.1–0.5°C/min are used.

The temperature rising elution step, which gives the name to the technique, can be performed at higher rates than the crystallization step and, typically, heating rates (HR) of 0.5–5°C/min are used. Most important is to relate the heating to the flow rate used, as discussed above with (3). A slow HR with a high flow rate would elute polymer fractions in a large solvent volume and therefore with a reduced signal-to-noise ratio whereas a low flow rate and fast HR would result in a too-concentrated solution going through the column, which may result in plugging (besides loss in resolution, as discussed later in this section). Typically, flow rates of 0.5–2 mL/min are used depending on the HR being used, and are optimized for column dimensions and sample size.

The TREF elution curve resembles a chromatogram with a small peak at the beginning (typically obtained at isothermal elution), which corresponds to the fraction that has not crystallized at the lowest crystallization temperature chosen in the analysis method; this is followed by the continuous elution of the fractions of increasing crystallinity as temperature rises (as shown in Fig. 15). Cooling down

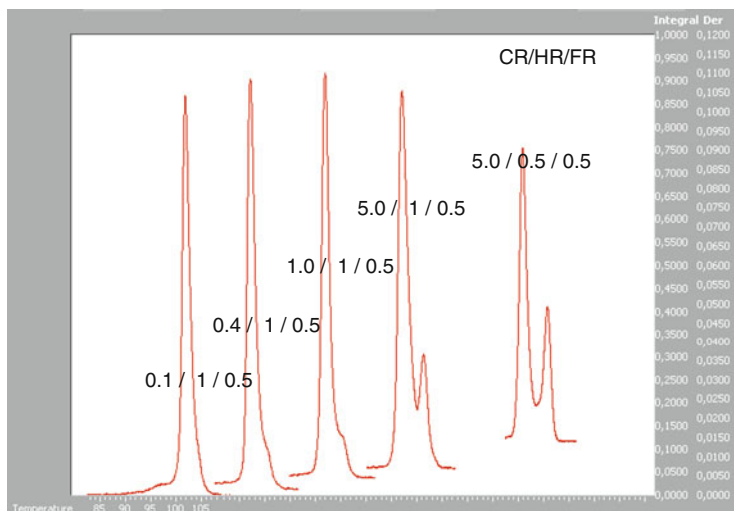


Fig. 16 TREF analysis of HDPE resin. Appearance of a double peak artifact by melt and re-crystallization phenomena

the solution to very low temperatures to achieve the overall crystallization of the sample is not always practical and, quite often, with low crystallinity samples it is not possible to reach it before the solvent itself crystallizes. In those cases, a more precise representation of the CCD is shown in Fig. 15, where the continuity of the CCD is represented down to the lowest temperature analyzed and the remaining soluble fraction is represented by a rectangle with the corresponding surface area at the lowest analysis temperature.

In TREF analysis, with a finite and usually large sample solution volume (V) injected into the column, there is a physical limit to the maximum resolution achievable, which we have defined as geometric dispersion (gd) [90], given by (4):

$$gd = HR \cdot V/F, \quad (4)$$

which corresponds to the temperature range in which the same type of polymer molecules are going to be eluted at a given heating rate HR and flow rate F . For a sample volume of 0.5 mL injection (assuming that it will be diluted into the column to double that volume) and using a HR of $1^\circ\text{C}/\text{min}$, a flow rate of 1 mL/min or higher is required to achieve a gd of 1°C or lower, which is acceptable given the intrinsic low resolution of the TREF technique. The low HR/F ratios required to achieve the lowest gd in (4) compete with the high HR/F ratios demanded by (3) to have good detector response.

The use of faster crystallization rate in TREF may result in formation of metastable crystals that re-crystallize during the heating cycle and result in anomalous double peaks, as shown in Fig. 16 for the analysis of an HDPE resin at different crystallization and heating rates. Increasing the heating rate can also overcome this effect by not giving time for re-crystallization.

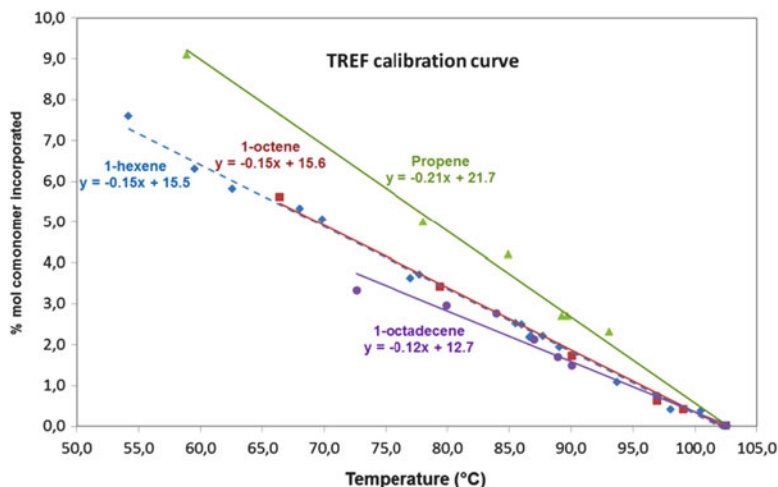


Fig. 17 TREF calibration with copolymers of different type of branches [92]

To reduce co-crystallization in polypropylene, Iiba et al. [91] proposed a temperature cycling scheme during crystallization, which they implemented in a home-made TREF using a narrow bore TREF column.

TREF analysis is still reported quite often on the basis of dissolution temperature scale, but as discussed in the introduction of Sect. 4.1 there is a linear relation between dissolution temperature and comonomer incorporation, which has been confirmed experimentally [62]. The calibration of temperature to comonomer content can be performed by using narrow composition standards (metallocene-type resins) of the same comonomer type. Boisson et al. [92] recently presented TREF calibration curves for different types of PE copolymers, as shown in Fig. 17. At the same mole percentage of comonomer incorporated, the dissolution temperature (TREF) decreases with increasing branch length. Propylene incorporation in PE with the lowest short chain branch (methyl), results in the highest dissolution temperature indicating that the methyl branch, besides being able to enter into the crystal lattice, has the lowest crystallizability perturbation. Octene and hexene copolymers can use the same calibration curve as shown in Fig. 17.

The elution order in TREF has been shown to be independent of molar mass above 10,000 g/mol [61, 62]. On the other hand, it has been shown that in the case of single-site catalyst resins the lowest molar mass results in broader composition distributions [93], as expected for purely statistical reasons [94].

The CCD curve shown in Fig. 15 contains all the information on composition distribution and it is a common practice to compare the CCD curves of the different resins to be evaluated: In addition to the CCD curve, it is convenient to work with some easy-to-use average parameters. In the case of multiple peaks (like those shown in Fig. 15), integration of the peaks is most appropriate. In bimodal LLDPE, the most important parameters to measure are the homopolymer (linear) and soluble fraction percentages. Calculation of moments similar to

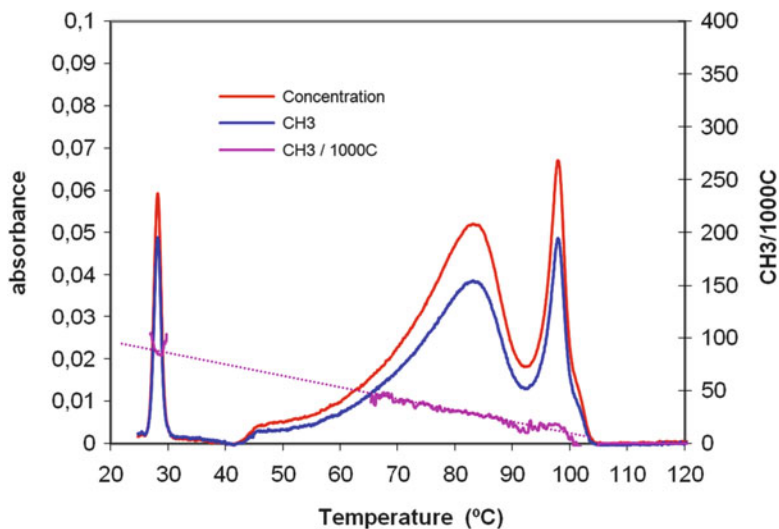


Fig. 18 TREF analysis of a LLDPE with IR detection and composition sensor. The *straight line* corresponds to the calibration curve for CH₃/1000C versus elution temperature obtained with the integrated composition sensor

average M_n and M_w values can also be practical [84], in terms of temperature or comonomer mole percentage (when calibration is performed) as shown with (5–7):

$$T_n = \frac{\sum c_i}{\sum c_i/T_i}, \quad (5)$$

$$T_w = \frac{\sum c_i \cdot T_i}{\sum c_i}, \quad (6)$$

$$r = \frac{T_w}{T_n}. \quad (7)$$

Other parameters have been proposed in the patent literature to describe the CCD, such as the composition distribution breadth index (CDBI), defined as the weight percentage of the copolymer molecules having a comonomer content within 50% of the median total molar comonomer content [95], or the solubility distribution breadth index (SDBI), which is analogous to the standard deviation of the CCD [96].

The possibility to incorporate a composition sensor in the TREF IR detector has been shown by Monrabal [97]. Two simultaneous signals are obtained, one for total concentration and a second signal emphasizing the methyl absorption in a similar way as discussed for GPC in Fig. 8. The ratio of the two signals measures the CH₃/1000C value, as shown in Fig. 18, which in the case of a PE resin analysis corresponds in fact to the TREF calibration curve and shows a linear dependence on temperature.

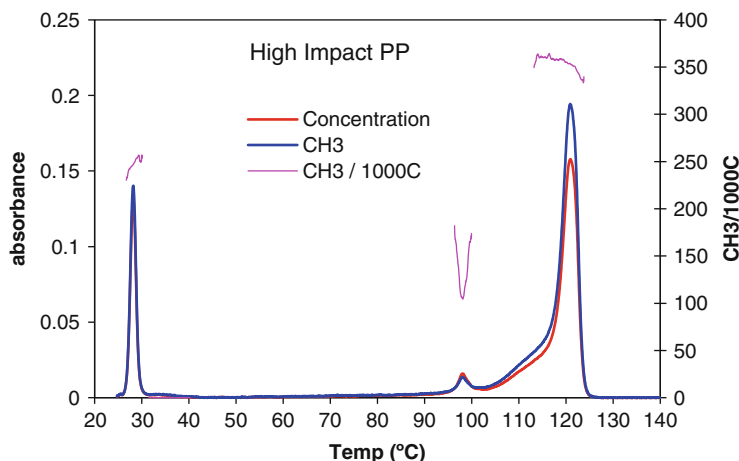


Fig. 19 TREF analysis of a high impact polypropylene. The small peak at 98°C corresponds to PE homopolymer, as deduced from the CH₃/1000C signal

The incorporation of a composition sensor is important when analyzing PP copolymers because both tacticity and branching play a role in the separation by crystallizability, as discussed in Sect. 2.2. The analysis of a high impact PP copolymer is shown in Fig. 19, where a small peak of linear PE on the tail of the PP curve is easily identified by the sudden change in methyl content.

Besides concentration and composition sensors, viscometer and/or light scattering detectors can be added to a TREF apparatus, as shown in Fig. 14, thus obtaining information on composition–molar mass interdependence, which is of important value when analyzing complex multireactor resins. An example of a TREF analysis of a complex resin with both detectors is shown in Fig. 20, where it can be seen that the less crystalline fraction is of higher molar mass than the more crystalline fraction.

TREF has also been used in the mathematical modeling of PE copolymers, as shown by Soares et al. [98].

4.1.3 Crystallization Analysis Fractionation

Crystallization analysis fractionation (CRYSTAF) was developed by Monrabal [99] in 1991 as a process to speed up the analysis of the CCD, which at that time lasted around 1 week per sample with the TREF technique. CRYSTAF shares with TREF the same principle of separation according to crystallizability. In CRYSTAF, the samples are not crystallized in a column but in a stirred vessel with no support, and only a temperature cycle (crystallization) is required [64], thus speeding up the analysis process and simplifying the hardware requirements.

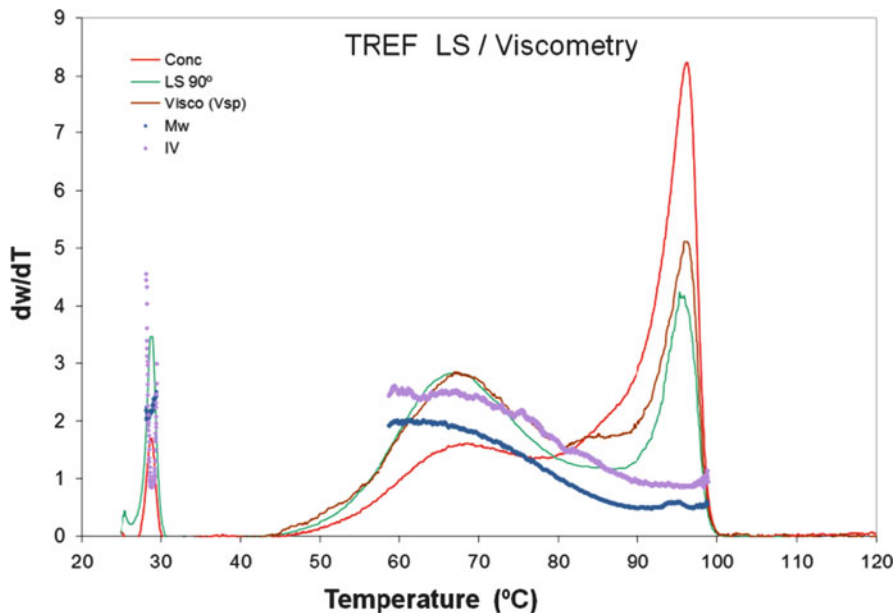


Fig. 20 TREF analysis of a complex resin with light scattering (*LS*) and viscometer (*visco*) detectors; *IV* intrinsic viscosity

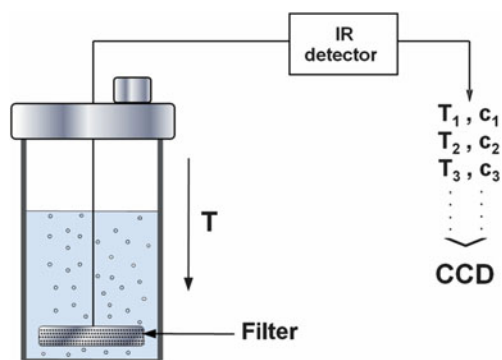


Fig. 21 CRYSTAF sampling process in a vessel with an internal filter; *T* temperature, *c* concentration

In CRYSTAF, the analytical process is followed by monitoring the polymer solution concentration during crystallization by temperature reduction. Aliquots of the solution are filtered (through an internal filter inside the vessel) and analyzed by a concentration detector at different temperatures, as shown in Fig. 21. The whole process is similar to a classical stepwise fractionation by precipitation with the exception that, in this new approach, no attention is paid to the polymer being precipitated but to the one that remains in solution.

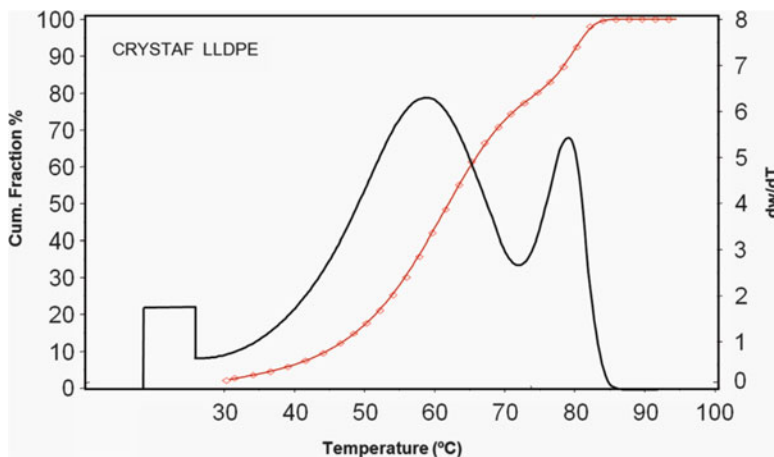


Fig. 22 CRYSTAF cumulative data points (*circles*) and the first derivative CCD curve

The first sampling points, taken at high temperatures where all polymer remains in solution, provide a constant concentration equal to the initial polymer solution concentration, as shown by the flat part of the cumulative curve in Fig. 22. As the temperature drops the most crystalline fractions, composed of molecules with less irregularities (high crystallinity), will precipitate first, resulting in a steep decrease in the solution concentration on the cumulative plot. This is followed by precipitation of fractions of increasing irregularities or branch content (lower crystallinity) as the temperature continues to drop; the last data point, which corresponds to the lowest temperature of the crystallization cycle, represents the polymer fraction that has not crystallized (mainly highly branched or amorphous material) and remains in solution at that temperature. The first derivative of this curve, shown in Fig. 22 (in this example being a LLDPE resin), corresponds to the CCD when the temperature scale is calibrated in number of branches per 1,000 carbon atoms. With this approach, the CCD can be analyzed in a single crystallization cycle without physical separation of the fractions. The term “crystallization analysis fractionation” (CRYSTAF) stands for this process.

The way the analysis is performed, by using a discontinuous sampling process while the crystallization proceeds, provides the possibility to easily automate the technique, as shown in Fig. 23 where five different samples introduced in separate crystallization vessels can be analyzed simultaneously.

During the crystallization cycle, all the vessels are “sampled” many times in a sequential manner and at the end of the analysis there are enough temperature–concentration data points for each resin to properly draw the cumulative curves, as shown in Fig. 24, with the simultaneous analysis of five LLDPE resins of different density. The complete dissolution and crystallization analysis of five samples can be carried out simultaneously in around 7 h in a fully automated way.

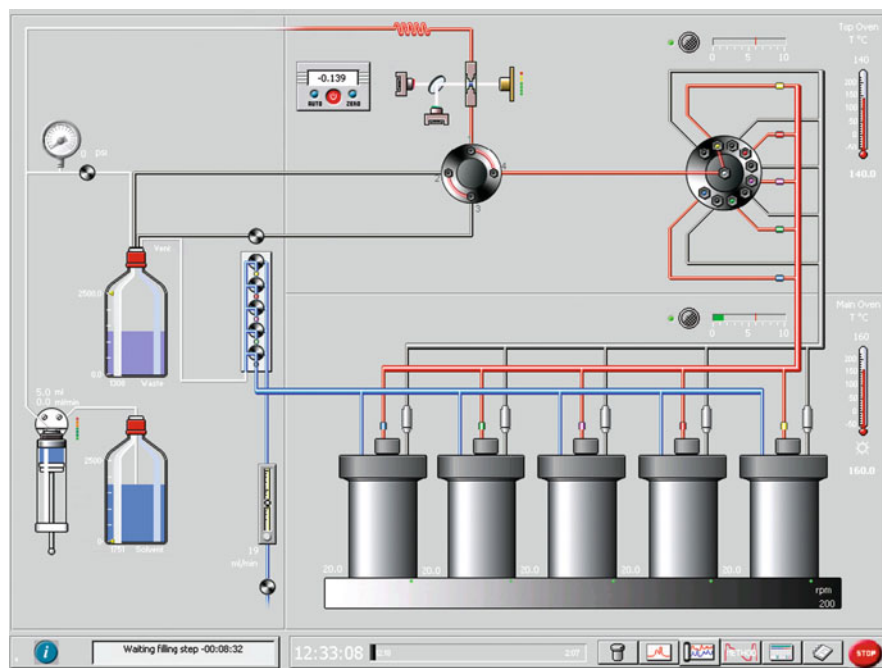


Fig. 23 CRYSTAF instrument

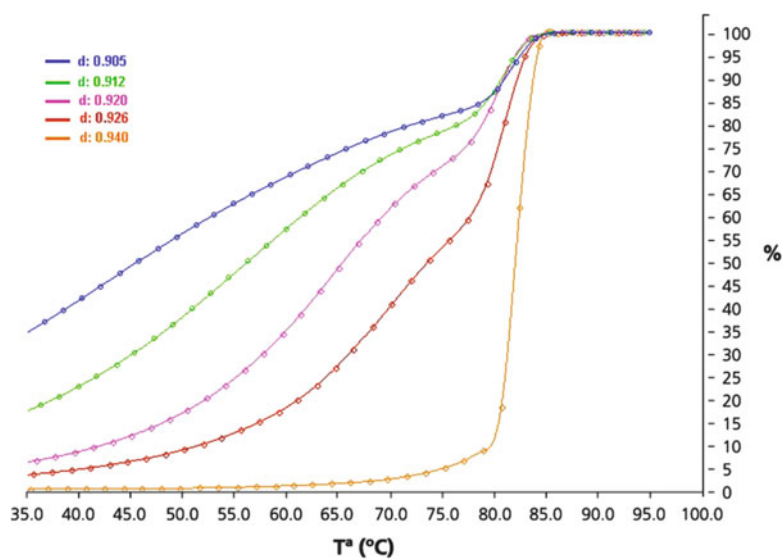


Fig. 24 Simultaneous CRYSTAF analysis of five LLDPE resins of different density (cumulative curves). 40 mg/40 mL in TCB; crystallization rate $0.2^{\circ}\text{C}/\text{min}$

The same solvents, same IR detector and similar calculation parameters to those presented in Sect. 4.1.2 for TREF are applicable for CRYSTAF analysis. The calibration of temperature to comonomer content can be performed by using narrow composition standards (metallocene-type resins) of the same comonomer type, with similar results to TREF as discussed in Sect. 4.1.2. Octene and hexene copolymers follow the same calibration curve [92].

Reviews of the CRYSTAF technique and applications have been presented [80, 83, 84]. Mathematical modeling of CRYSTAF crystallization kinetics has also been investigated [100].

Comparison of TREF and CRYSTAF

Both techniques share the same principles of fractionation on the basis of crystallizability. TREF is carried out in a packed column and demands two full temperature cycles, crystallization and elution (dissolution), to obtain the analysis of the composition distribution. In CRYSTAF, the analysis is performed in a single step, the crystallization cycle, which results in faster analysis time and simple hardware requirements.

TREF has the advantage that a continuous elution signal is obtained and molar mass detectors can be easily added to obtain composition molar mass interdependence; an autosampler can also be added for multiple sample analysis. CRYSTAF takes advantage of discontinuous sampling to analyze a set of samples simultaneously.

Both techniques provide similar results; the comparison of TREF and CRYSTAF has already been discussed [84] and the most significant difference is the temperature shift due to the undercooling, as analytical conditions are far from equilibrium; CRYSTAF data are obtained during the crystallization whereas TREF data are obtained in the melting-dissolution cycle. Both techniques, however, can be calibrated and the results expressed in branches/1000C will be similar for PE copolymers.

The large difference in undercooling between polypropylene and polyethylene makes the analysis of complex resins containing both PE and PP an interesting case, whereby both TREF and CRYSTAF must be used to obtain unequivocal results, as discussed in a recent publication [101]. TREF, which analyzes samples in the dissolution (melting), provides best resolution for the analysis of blends containing isotactic polypropylene and polyethylene; on the other hand, CRYSTAF, which obtains the data during the crystallization, is the preferred technique when analyzing combinations of polyethylene with ethylene-propylene copolymers resins, as seen in Fig. 25.

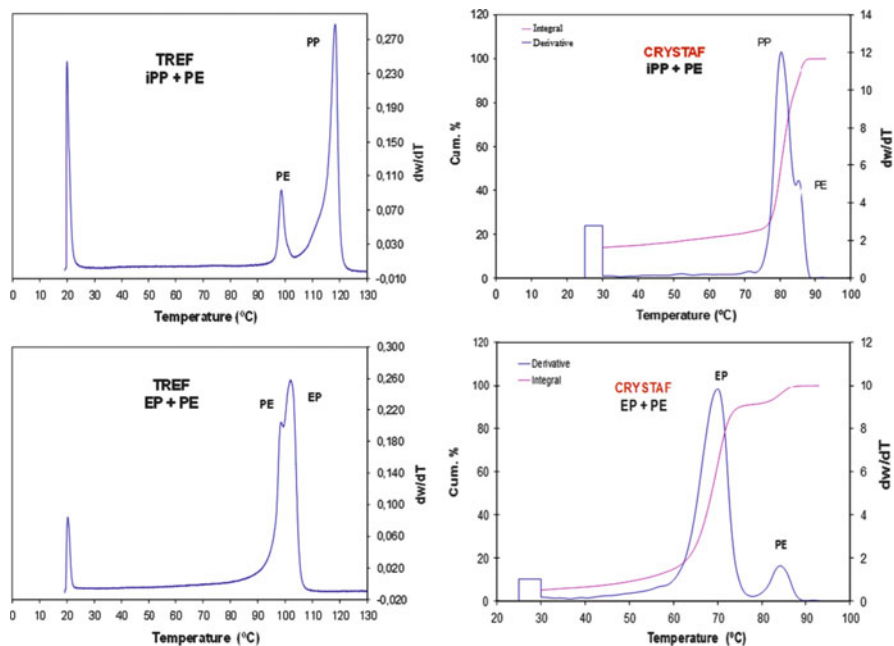


Fig. 25 TREF and CRYSTAF analysis of PE-PP combinations. TREF separates iPP + PE better and CRYSTAF separates EP + PE better

4.1.4 Crystallization Elution Fractionation

Crystallization elution fractionation (CEF) is a new separation technique developed by Monrabal [102] for the analysis of the CCD that combines the separation power of CRYSTAF and TREF. The CEF technique is based on a new and patented separation principle, referred to as dynamic crystallization (DC) [87], that separates fractions inside a column according to crystallizability while a small flow of solvent passes through the column. The separation by DC occurs during the crystallization step. CEF combines the separation power of DC in the crystallization step with the separation during dissolution of the TREF technique.

The principles of DC and CEF are presented in Fig. 26 and compared with classical TREF analysis. In TREF, the crystal aggregates formed during crystallization from the various composition families in the resin are all mixed together at the column spot where the sample was loaded. In Fig. 26a, the three different composition families crystallized in this example are deposited at the head of the column with no physical separation of the corresponding molecules. The physical separation in TREF takes place in the elution cycle.

CEF analysis follows similar steps as in TREF, but during the crystallization cycle a small solvent flow, FC, is passed through the column in such a way that when molecules of a given composition reach their crystallization temperature, they are segregated from solution and anchored on the support. Meanwhile, the

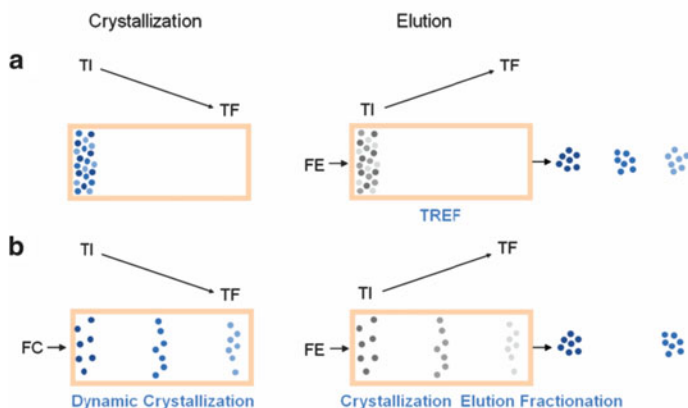


Fig. 26 Separation by crystallizability: (a) TREF separation process, (b) dynamic crystallization and crystallization elution fractionation. TI initial crystallization and elution temperatures, TF final crystallization and elution temperatures, FE elution flow, FC crystallization flow

other components of lower crystallinity, still in solution, move along the column until they reach their own crystallization temperature. At the end of the crystallization cycle, the three composition families shown in Fig. 26b are physically separated inside the column according to crystallizability; this process is referred to as dynamic crystallization and can separate components in a similar fashion as CRYSTAF although all polymer molecules still remain inside the column in three different locations.

Once the DC separation step has been completed, it is easy to realize the possibility to combine it with a final elution cycle as in TREF to obtain a new *extended* separation as shown in Fig. 26b by the improved separation of the three components at the exit of the column in CEF analysis as compared to the TREF approach. It is quite interesting that the separation power of CRYSTAF and TREF are combined in CEF when both systems are based on the same crystallizability principles. To obtain the maximum benefit of the DC process, the column volume must be large enough and the flow rate in the crystallization (FC) has to be adapted to the crystallization rate (CR), crystallization temperature range (ΔT_c) of the components to be separated, and column volume (V) as described by (8):

$$FC = \frac{V}{\Delta T_c} \times CR. \quad (8)$$

The calculated flow FC implies that all the components will be separated along the whole length of the column.

The CEF instrument is similar to an HPLC or TREF apparatus, as shown in the schematic diagram of Fig. 27; the main CEF characteristic is the ability to provide a small controlled flow during the crystallization process.

CEF has been shown to provide reproducible and very fast analysis of the composition distribution of polyolefins for high-throughput applications [87], as

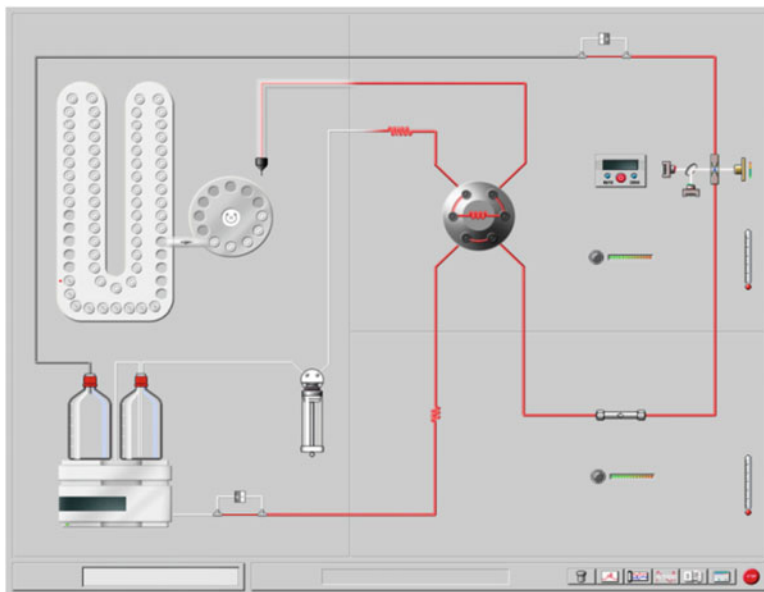


Fig. 27 CEF/TREF apparatus with autosampler

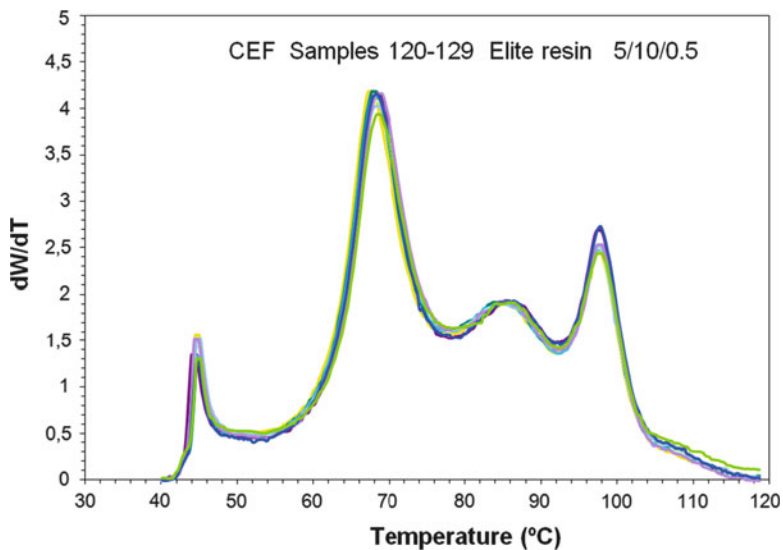


Fig. 28 Multiple CEF analysis ($\times 10$) of an Elite resin obtained at crystallization rate of $5^\circ\text{C}/\text{min}$ and heating rate of $10^\circ\text{C}/\text{min}$; injection volume, $20\ \mu\text{L}$ of $0.5\% \text{w/v}$; elution flow, $0.5\ \text{mL}/\text{min}$; analysis time per sample, 25 min

shown in Fig. 28. The analysis of a complex multireactor LLDPE resin is completed in less than 30 min with reasonable resolution and good reproducibility, as shown by the repeated analysis (ten times) of the same sample.

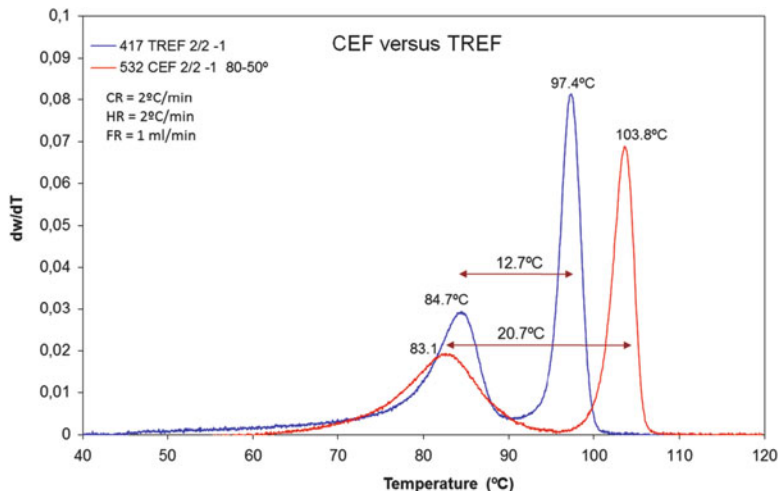


Fig. 29 CEF and TREF analysis of a 50/50 blend of two metallocene-type resins of very close density at 2°C/min cooling rate. Crystallization flow in CEF was 0.4 mL/min; elution flow in both CEF and TREF was 1 mL/min [90]

A comparison of techniques has shown a significant improvement in separation with CEF over TREF [90] when analyzing blends of very close comonomer content, as presented in Fig. 29. The importance of optimizing the DC step, responsible for the extended CEF separation, has been shown in this example. The better separation obtained in CEF as well as a lower co-crystallization can be interpreted by the combination of the two separation processes.

4.2 Chromatography-Based Techniques

The use of HPLC in the analysis of copolymers was already quite established in the 1990s [103, 104]. A significant effort was demanded to apply this technique to the analysis of polyolefins because of the high temperatures required for the dissolution of the polymer and the new solvents and detectors needed for work under gradient conditions. It was the work of Professor Pasch's group at DKI (German Institute for Polymers, Darmstadt) during the last decade that established the basis of this new tool, which is sometimes referred to as "interaction chromatography."

Most extensive work has been done by Macko et al. using a solvent gradient on silica- or carbon-based columns and using an evaporative light scattering detector (ELSD), as reviewed recently [105] and discussed in Sect. 4.2.1.

In recent years, a new approach by Cong et al. using a thermal gradient instead of a solvent gradient system on the same carbon-based column has demanded

significant attention because of the simplicity of the isocratic system and easy detection, as will be discussed in Sect. 4.2.2.

Both solvent gradient and thermal gradient systems have become new tools for characterizing copolymers in short analysis times and for extending the range of polymers to be analyzed towards the elastomers region that could not be characterized by crystallization techniques.

4.2.1 Solvent Gradient Interaction Chromatography

The use of a solvent/non-solvent approach to separating PE and PP in a preparative mode was shown by Lehtinen et al. [106] using ethylene glycol monobutyl ether (EGMBE) as a non-solvent. Macko et al. [107] were the first to implement this approach in analytical HPLC, using EGMBE as a mobile phase in an isocratic mode but depositing the polymer in the column with TCB; a separation of PE and PP was obtained but without full recovery of the PE resin. Heinz et al. [108], from the same group at DKI, used a solvent gradient approach (EGMBE-TCB) to achieve a separation of PE and PP (for PE of molecular weight higher than 50,000 g/mol) with full recovery of PE. A similar approach was used by Albrecht et al. [109] to separate EP copolymers and ethylene-vinyl acetate (EVA) resins [110], and by Dolle et al. [111] to characterize an LLDPE resin.

In all cases, an ELSD was the only possible detection system because of the solvent gradient. Pasch et al. [112] reported the separation of EVA and ethylene-methyl acrylate (EMA), and also combined the solvent gradient separation with collection of germanium disks for FTIR measurement.

A significant breakthrough came with the separation of polyolefins by adsorption on a carbon-based column (Hypercarb); Macko and Pasch [113] obtained a separation of isotactic, syndiotactic, and atactic polypropylene together with linear polyethylene using a gradient of decanol-TCB in a very short analysis time, as shown in Fig. 30.

Using the same Hypercarb column and eluents, Macko et al. have shown a separation of ethylene copolymers by the level of comonomer incorporation [114, 115]. Similar results were obtained by Miller et al. [116] on the same Hypercarb column. The presence of branches in the ethylene copolymers reduces the adsorption potential on the atomic level flat surface of graphite and a linear correlation is obtained between the comonomer mole percentage incorporated and the elution volume, as shown in Fig. 31 for various types of copolymers.

Solvent gradient interaction chromatography (SGIC) can be used to analyze copolymers in the whole range of 0–100% of comonomer incorporation, which was not possible with crystallization techniques.

The combination of SGIC with SEC in a second dimension (SGIC2D) was shown by Roy et al. [117] using a gradient of decanol or EGMBE and TCB on a Hypercarb column; a second dimension with the standard GPC columns and isocratic TCB solvent was used with IR detection. Besides the convenience and linearity of the IR detector, the molar mass–composition interdependence could be

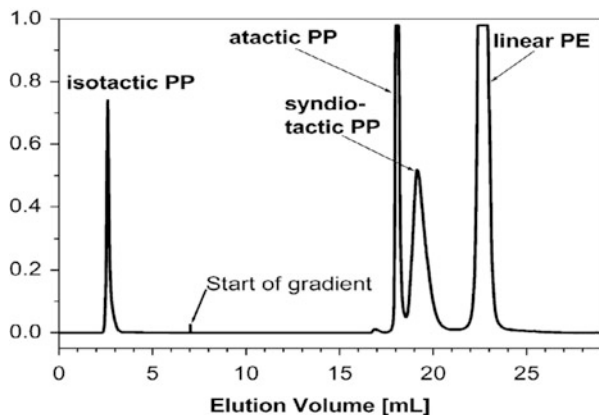


Fig. 30 SGIC analysis of polyethylene and polypropylenes of different tacticity on a Hypercarb column [113]

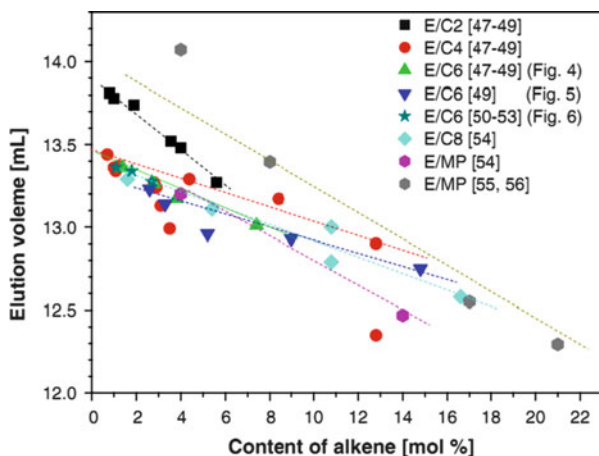


Fig. 31 Analysis of different ethylene copolymers by interaction chromatography on a Hypercarb column [115]

analyzed as shown in the analysis of ethylene octene copolymers in Fig. 32. Another advantage of SGIC2D is that a light scattering or viscometer detector could be added in the second isocratic dimension.

Ginsburg et al. [118] have used SGIC2D for the characterization of ethylene propylene and ethylene propylene diene (EPDM) rubbers; the technique provides a new approach to full characterization of resins in terms of composition–molar mass interdependence that cannot be fully analyzed by TREF-GPC because of the low crystallinity of the resins. Cheruthazhekatt et al. [119] have used SGIC2D together with other techniques to fully characterize high impact polypropylene. The SGIC technique attracted interest at the recent International Conference on Polyolefin Characterization (ICPC, Houston, October 2012), with general

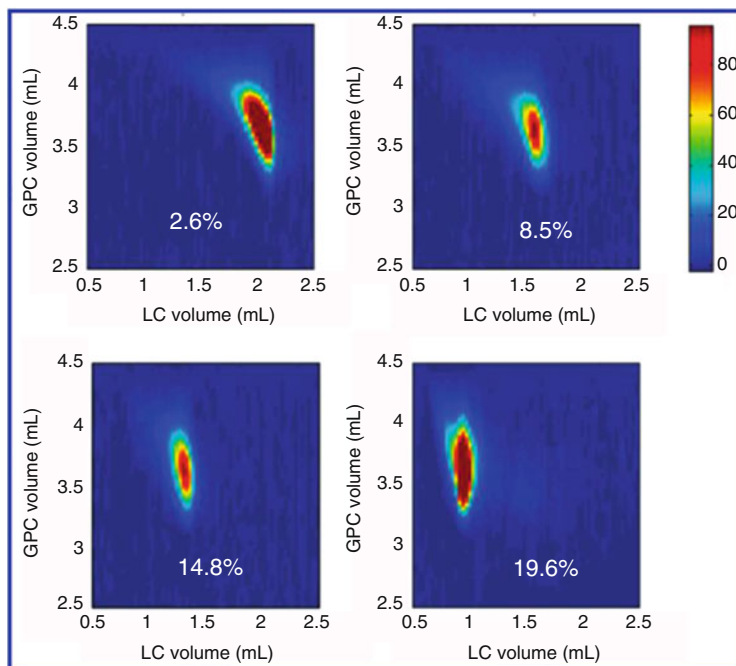


Fig. 32 SGIC2D analysis of ethylene octene copolymers [117]

papers from Pasch and Brüll, investigations on the graphite porosity influence on the separation mechanisms by Mekap, and combinations of SGIC with DSC and FTIR by Cheruthazhekatt.

4.2.2 Thermal Gradient Interaction Chromatography

Solvent gradient HPLC can be successfully replaced by thermal gradient using reverse phase columns to analyze copolymers, as shown by Chang et al. [120]. At the 3rd International Conference on Polyolefin Characterization in 2010, Cong et al. [121] showed the possibility of using the Hypercarb column with a thermal gradient for the analysis of ethylene copolymers [122]. The separation obtained was similar to the results previously discussed in SGIC but in this case at isocratic conditions, which allowed the use of a linear IR detector as well as an in-line viscometer or LS molar mass detection. The separation of a series of ethylene octene copolymers covering a broad range of comonomer incorporation is shown in Fig. 33. A linear relation is obtained between elution time and mole percentage of comonomer incorporation, and elution is independent of molar mass for molecular weights higher than 20,000 g/mol.

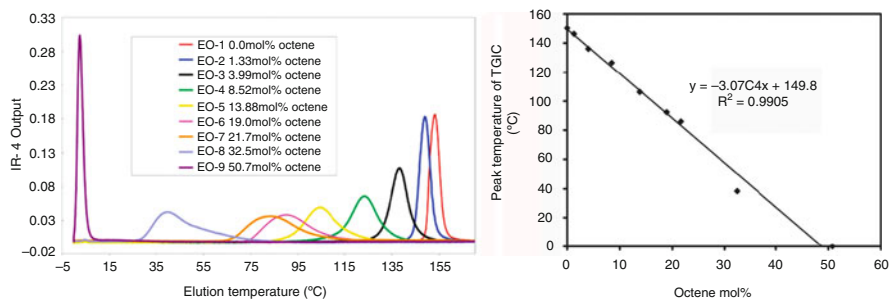


Fig. 33 TGIC analysis of a series of octene copolymers on a Hypercarb column (*left*) and calibration curve (*right*) [122]

The comparison of TGIC and TREF for a series of ethylene octene copolymers has been reported by Monrabal et al. [123], showing that resolution on TREF is slightly better than TGIC. TGIC, however, does not suffer from co-crystallization effects and covers a broader copolymer range down to the elastomer region, which crystallization techniques cannot reach.

Cong et al. [124, 125] have shown that other graphitized carbon packings provide similar results to those of Hypercarb. Monrabal [126] explained the separation mechanism on graphite by weak van der Waals forces and steric hindrance on an atomic-level flat surface like graphene, where the chemical structure of graphene should not be as important for interaction with the non-polar polyolefins; this was confirmed by using other types of layered packing materials like molybdenum sulfide, which provided the same separation order as the Hypercarb column [126, 127] in spite of totally different surface chemistry and polarity, as shown in Fig. 34 for a series of ethylene octene copolymers. The peaks were broader in the molybdenum sulfide column due to the broad particle size used as compared to the Hypercarb narrow particle size packing.

Other layered packings like boron nitride and tungsten sulfide showed adsorption and similar selectivity for ethylene copolymers and polypropylenes as the Hypercarb packing [126, 127] shown in Fig. 35, whereas the TREF column with metal shots or glass beads (but non-layered packings) separated by crystallization at significantly lower temperatures.

The speed and simplicity of the TGIC technique together with the possibility of using multiple detectors are of great significance for the characterization of polyolefins, especially in the elastomers region, and has attracted attention, with various papers being presented at the recent International Conference on Polyolefins Characterization (ICPC, Houston October 2012), which will be published in a forthcoming Macromolecular Symposia book. Cong [125] reported the application of TGIC in the analysis of block copolymers and emphasized the use of triple detector in the analysis by TGIC. Monrabal [127] presented the separation on non-carbon packings like molybdenum sulfide and boron nitride, proposed a new separation mechanism on atomic-level flat surfaces packings, and showed that addition of polar solvents did not change the selectivity of adsorption on those layered packings by TGIC. An explanation for the unusual elution of iPP in TGIC

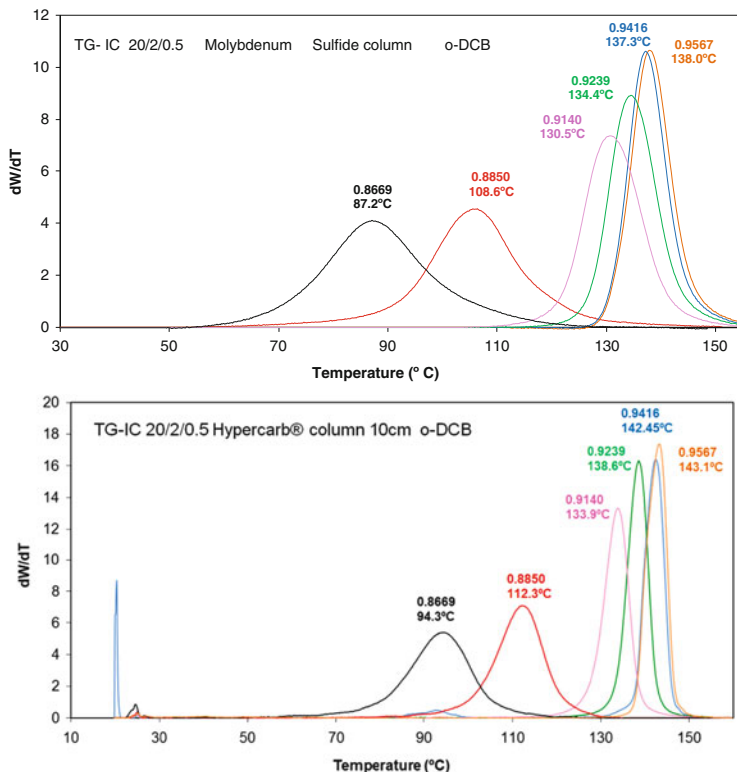


Fig. 34 TGIC analysis of a series of octene copolymers on Hypercarb and molybdenum sulfide [126]

was provided, i.e., that the adsorption of iPP on Hypercarb or other layered packings is so weak that polymer crystallizes at a higher temperature than that at which adsorption occurs, and thus iPP is eluted in TREF mode.

5 Bivariate Distribution: Characterization Techniques

The CCD and the MWD are the most relevant microstructure parameters of a polyolefin resin with a given comonomer type. There are other features, however, that need to be characterized such as LCB and its distribution or the intramolecular homogeneity, but most important for full characterization of a classic polyolefin resin is analysis of the dependence of molecular mass on composition, also known as the bivariate distribution.

For many years the only possibility to measure the bivariate distribution was by preparative fractionation followed by analysis of the fractions by the second

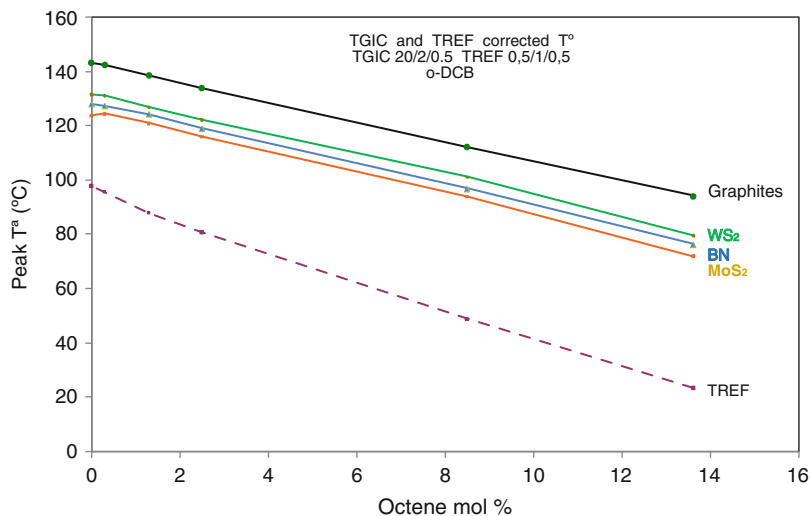


Fig. 35 TGIC analysis of a series of octene copolymers on different adsorbents and comparison with a TREF column [127]

dimension technique. In that case there are two possible analytical routes to perform the cross-fractionation:

1. To first fractionate the polymer on the basis of molecular mass followed by composition analysis (TREF)
2. To first fractionate the polymer on the basis of composition (TREF) followed by molar mass analysis (GPC)

Aust et al. [128] have used the molar mass fractionation first on a medium density polyethylene, and Faldi and Soares [129] the composition fractionation first on an LLDPE resin. One should choose the fractionation technique that results in the most discriminated fractions [80] in the first step. The most general approach is to use preparative TREF fractionation because the CCD is usually more discriminating than the MMD in complex polyolefins.

A major achievement in automation was done by Nakano and Goto [130], who combined a TREF with a GPC as early as 1981 and presented the full information of the bivariate distribution in three dimensional (3D) plots (contour maps or bird's-eye views) as shown in Fig. 36.

More recently, Li Pi Shan et al. [131] built a home-made TREF-GPC cross-fractionation apparatus, which was later modified by Gillespie et al. [132] to perform GPC-TREF as well. However, in subsequent years the TREF-GPC combination has been the preferred mode of operation.

A commercial TREF-GPC bench-top apparatus was developed by Polymer Char in collaboration with Mitsubishi Petrochemical in 2005. A description of the technique is given by Ortín et al. [133] and a schematic diagram is shown in Fig. 37.

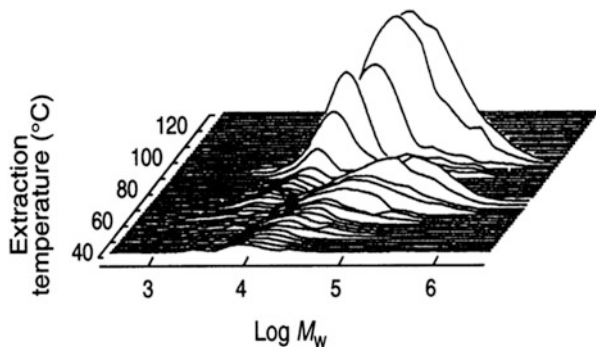


Fig. 36 TREF-GPC [130]

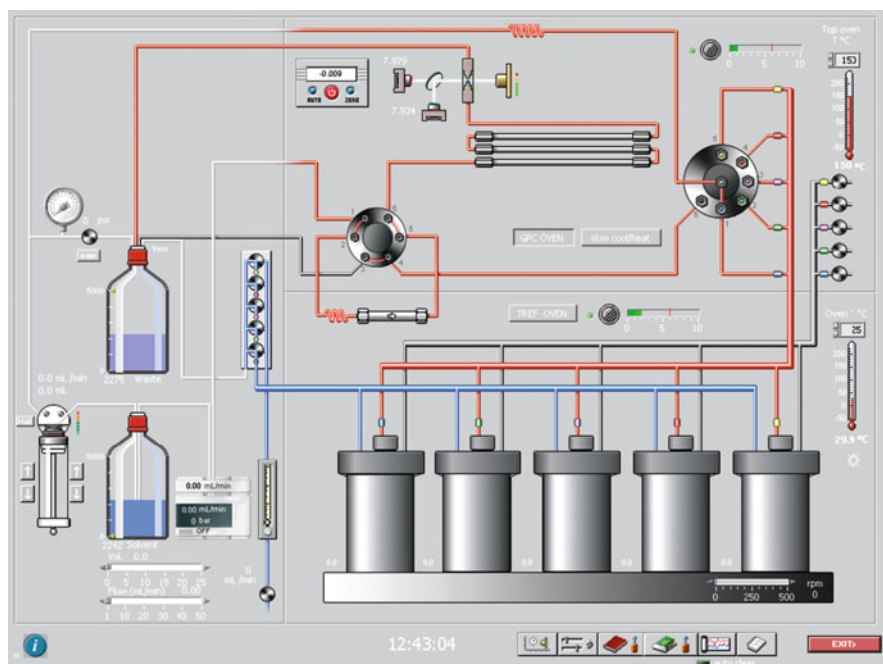


Fig. 37 Cross-fractionation instrument TREF-GPC

The sample is dissolved automatically and loaded into the TREF column to undergo crystallization. The temperature rising elution is performed in isothermal steps, as shown in Fig. 38, and at each temperature step the column is washed and the solution injected into the GPC columns, in this particular example being an LLDPE resin.

Cross-fractionation analysis performed with a sufficient number of isothermal steps (high resolution) takes a longer time but provides unexpected views of the

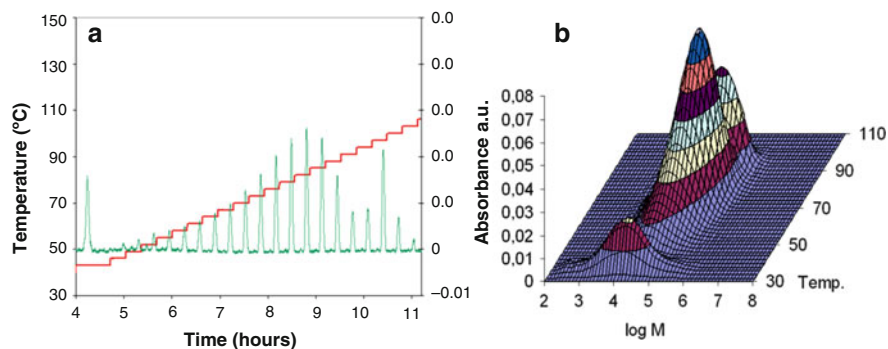


Fig. 38 (a) TREF isothermal steps with GPC obtained at each temperature. (b) 3D plot of the reconstructed bivariate distribution of an LLDPE resin

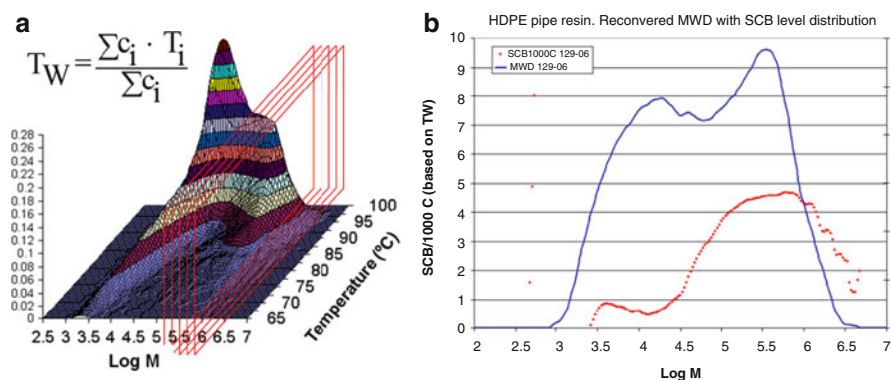


Fig. 39 (a) High resolution cross-fractionation (TREF-GPC) of a pipe resin and (b) reconstructed MMD with comonomer content plotted against the molar mass (M)

polymer structure [133], as shown by the analysis of a bimodal pipe resin in Fig. 39. By calculating the average temperature of each slice in the temperature axis and transferring the value to methyls per thousand carbons, the 2D view could be reconstructed with similar results to those obtained by GPC-IR, as shown in Fig. 39b.

The TREF-GPC analysis can be performed with an additional composition sensor (CH_3 sensor), as discussed in previous sections. This is especially important for ethylene propylene copolymers or blends since crystallizability is influenced in the case of PP by both tacticity and ethylene incorporation, as discussed for Fig. 4. The composition sensor provides a means to assign the crystallization temperature to one or the other polymer. The analysis of a high impact PP containing a significant amount of PE homopolymer is shown in Fig. 40. A small peak eluted before the iPP is clearly associated with PE by having a significantly lower methyl content than the overall concentration response. The PE peak is eluted on the tail of the iPP where other EP species are also eluted (as discussed with Fig. 19) and the molar mass of the PE peak could be differentiated from the polypropylene part.

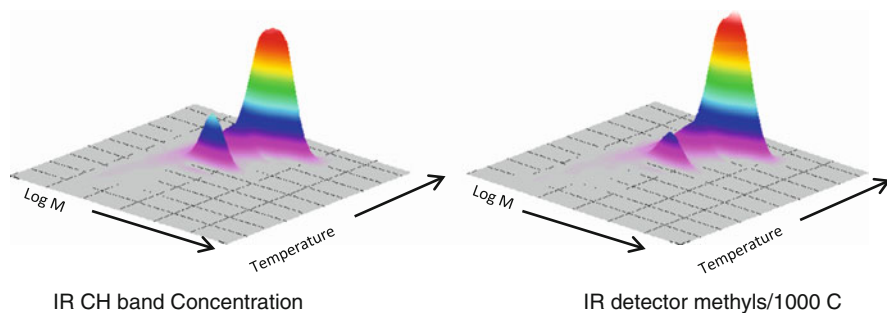


Fig. 40 TREF-GPC of a high impact PP with a significant amount of PE homopolymer. The analysis was performed with an additional CH₃ sensor. The amorphous fraction was not analyzed

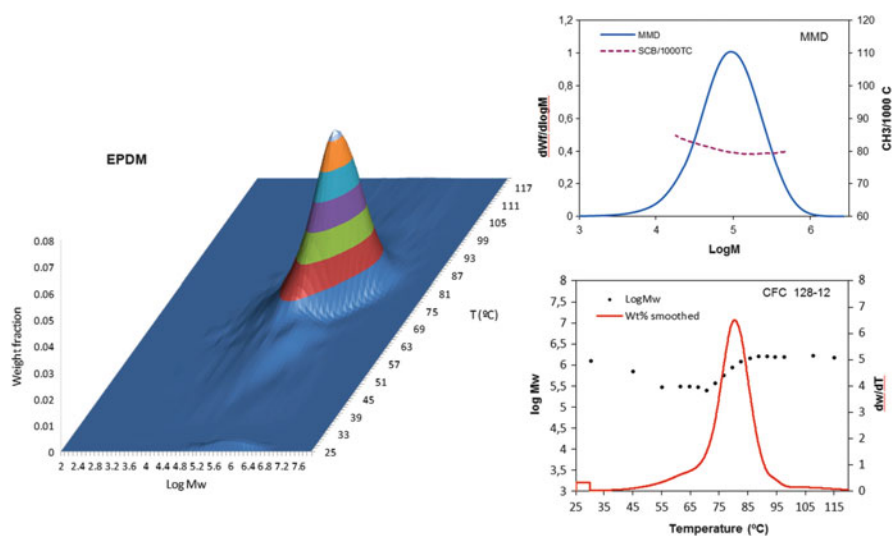


Fig. 41 Left: TGIC-GPC of an EPDM sample. Right: Reconstructed CCD and MMD with second dimensions

Besides TREF-GPC, we discussed in Sect. 4.2.1 that SGIC with a carbon-based column combined with GPC (SGIC2D) could also provide composition–molar mass interdependence [117, 118]. When dealing with more amorphous polymers, the interaction chromatography modes SGIC or TGIC are the most appropriate.

Quite interestingly, the combination of TGIC and GPC can be performed in the same instrument as the TREF-GPC; it only requires to replace the TREF column with the TGIC one. This is especially interesting given the method simplicity of the TGIC and TREF modes, with no requirement for a solvent gradient and easier availability of detectors than for the SGIC approach.

The analysis of an EPDM sample by TGIC-GPC is shown in Fig. 41 [134]. The amorphous EPDM polymer would not crystallize in TREF but it is adsorbed

on a atomic-level flat surface like carbon or molybdenum sulfide. The desorption volumes at increasing isothermal steps are injected into the GPC column, to obtain the composition–molar mass interdependence in a 3D plot or the 2D projections on the molar mass or composition curves of Fig. 41.

6 Summary, Conclusions, and Outlook

Polyolefins account for more than 50% of all synthetic polymers being produced today. The volume and applications of polyolefins have been substantially growing since the time of the Ziegler and Natta discoveries. With the introduction of metallocene and other single-site catalysts, polyolefins, with the simple chemistry of carbon and hydrogen, have evolved into complex microstructures that can be designed through multiple reactor–catalyst processes to achieve a desired performance for specific applications.

The characterization of the new polyolefins necessarily demands a separation step of the polymer by certain parameters and, in most cases, a cross-fractionation is required to obtain the full bivariate distribution. Other features like long chain branching and stereoregularity need to be characterized as well and eventually as a function of molar mass.

Molar mass distribution is a dominant microstructure parameter that, in copolymers, needs to be measured with additional information to account for long chain branching, comonomer incorporation, or ethylene propylene combinations (in the case of EP copolymers). The combination of GPC and IR spectroscopy has been shown to be of great value in the characterization of copolymers. The importance of automation and sample care, especially in the case of polypropylene, has been discussed as well as the significant improvement in sensitivity by the use of IR MCT detectors. There are big expectations for the analysis of ultrahigh molar mass polyolefins by the new AF4 technology.

Chemical composition distribution has become the most significant microstructure parameter in the new complex polyolefins, where different polymer families are often part of the same resin. Crystallization techniques are the most used for measurement of the CCD and a new technique, CEF, has been shown to be of value for high-throughput applications, with CCD measurements in less than 1 h. Crystallization techniques can be combined with viscosity and light scattering detectors to obtain the composition–molar mass interdependence.

The most recent development in separation is the development of high temperature interaction chromatography, which extends the composition distribution analysis to polyolefin copolymers of very low crystallinity, which is not possible to analyze by crystallization techniques. The analysis of complex polymers with different composition can be analyzed in a short time by solvent gradient interaction chromatography, SGIC, on an atomically flat surface like carbon or molybdenum sulfide packing. The addition of a second separation step by GPC (SGIC2D) provides the capability to obtain full composition–molar mass dependence.

Thermal gradient interaction chromatography (TGIC), with same type of columns as with SGIC, has been shown to be a very attractive variation because of easier detection by IR and the possible use of integrated in-line molar mass detectors.

Cross-fractionation chromatography, separating in a first step by composition followed by molar mass, is a very powerful approach to obtaining the full bivariate distribution of classical polyolefins and the most complete characterization of complex resins. TREF-GPC, TGIC-GPC, and SGIC2D are the various modes that can be used to obtain the three-dimensional analyses. Although not covered in this review, one should not forget the value of preparative fractionation combined with other separation techniques to obtain the three-dimensional plots as well as intramolecular characterization by spectroscopic techniques.

References

1. Staudinger H, Heuer W (1930) Highly polymerized compounds XXXIII. A relation between the viscosity and the molecular weight of polystyrenes. *Ber dtsh Chem Ges B* 63:222–234
2. Ziegler K, Holzkamp E, Breil H, Martin H (1955) *Angew Chem* 67:426–541
3. Haenel M (2008) Historical sites of chemistry. Karl Ziegler. Max Planck Institute for Coal Research, Mülheim an der Ruhr
4. Hogan JP, Banks RL (1958) US patent 2,825,721
5. Hogan JP, Banks RL (1986) History of crystalline polypropylene. In: Seymour RB, Cheng T (eds) *History of polyolefins*. D Reidel, Dordrecht, pp 103–115
6. Sinn H, Kaminsky W (1980) *Adv Organomet Chem* 18:99
7. Kaminski W (2004) *J Polym Sci A Polym Chem* 42:3911–3921
8. Natta G (1955) *Makromol Chem* 16:213
9. Natta G, Danusso F (eds) (1967) *Stereoregular polymers and stereospecific polymerizations*. Pergamon, Oxford
10. Moore JC (1964) *J Polym Sci A2*:835–843
11. Giddings JC (1966) *Sep Sci* 1:123–125
12. Yau WW, Kirkland JJ, Bly DD (1979) *Modern size exclusion liquid chromatography*. Wiley, New York (2nd edn. with Striegel AM in 2009)
13. Provder T (ed) (1999) *Chromatography of polymers*. ACS symposium series, vol 731. ACS, Washington
14. Grubistic Z, Rempp R, Benoit H (1967) *J Polym Sci B* 5:753
15. Cheung P, Lew R, Balke S, Mourey T (1993) *J Appl Polym Sci* 47:1701–1706
16. Scholte T, Meijerink N, Schoffeleers H, Brands A (1984) *J Appl Polym Sci* 29:3763–3782
17. Drott EE, Mendelson RA (1970) *J Polym Sci A* 2(8):1361–1371
18. Cote JA, Shida M (1971) *J Polym Sci A* 2(9):421–430
19. Servotte A, De Bruille R (1975) *Die Makromolekulare Chemie* 116:203–212
20. Usami T, Gotoh Y, Takayama S (1991) *J Appl Polym Sci* 43:1859–1863
21. De Groot W, Wayne J, Hamre J (1993) *Chromatography* 648:33–39
22. Wang W, Kharchenko S, Migler K, Zhu S (2004) Triple-detector GPC characterization and processing behavior of long-chain-branched polyethylene prepared by solution polymerization with constrained geometry catalyst. *Polymer* 45:6495–6505
23. Yu Y, DesLauriers P, Rohlfing DC (2005) *Polymer* 46:5165–5182
24. Monrabal B, Yau W (2011) Engineering advances in high temperature GPC instrumentation. *The Column* 7(7):8–15

25. Cong et al (2007) In: Proceedings international symposium on polymer analysis and characterization (ISPAC), Crete, June 2007
26. Wong WS (2012) Application of high temperature chromatographic and viscometric techniques for the characterization of highly isotactic polypropylene samples. In: Proceedings 4th international conference on polyolefin characterization, Houston, October 2012
27. Monrabal B, Sancho-Tello J (2009) High temperature GPC analysis of polyolefins with infrared detection. In: The applications book, July 2009. LCGC Europe, Chester
28. Monrabal B, del Hierro P, Roig A (2012) Improvements in the sample preparation of polyolefins to prevent polymer degradation prior to GPC/SEC and CEF analysis. In: Proceedings 4th international conference on polyolefin characterization, Houston, October 2012
29. Wyatt Technology Corporation, Santa Barbara www.wyatt.com
30. Malvern Instruments Ltd, Worcestershire www.malvern.com/viscotek
31. Ross JH, Casto ME (1968) *J Polym Sci C* 21:143–152
32. Dawkins JV, Hemming M (1975) *J Appl Polym Sci* 19:3107–3118
33. Bosch JV, Ortín A, Monrabal B (1998) Development of a highly stable multiple wavelength IR detector for on-line GPC, CRYSTAF and TREF analysis. In: Proceedings International GPC Symposium, Arizona, October 1998, 633–640
34. Housaki T, Satoh K, Nishikida K, Morimoto M (1988) *Makromol Chem Rapid Commun* 9:525–528
35. Nishikida K, Housaki T, Morimoto M, Kinoshita T (1990) *J Chromatogr A* 517:209–217
36. Markovich RP, Hazlitt LG, Smith-Courtney L (1993) Chromatography of polymers. In: Provder T (ed) *Characterization by SEC and FFF*. ACS symposium series, vol 521. American Chemical Society, Washington
37. DesLauriers PJ, Rohlffing DC, Hsieh ET (2002) *Polymer* 43:159–170
38. DesLauriers PJ (2005) Measuring compositional heterogeneity in polyolefins using SEC/FTIR spectroscopy. In: Striegel A (ed) *Multiple detection in size exclusion chromatography*. ACS symposium series, vol 893. American Chemical Society, Washington
39. Piel C, Albrecht A, Neubauer C, Klampfl CW, Reussner J (2011) *Anal Bioanal Chem* 400:2607–2613
40. Albrecht A (2012) Multidimensional fractionation techniques for the characterisation of HDPE pipe grades. In: Proceedings 4th international conference on polyolefin characterization, Houston, October 2012
41. Montesinos J, Tarín R, Ortín A, Monrabal B (2006) In: Proceedings 1st ICPC conference, Houston, October 2006
42. Monrabal B, Sancho-Tello J, Montesinos J, Tarín R, Ortín A, del Hierro P, Bas M (2012) High temperature gel permeation chromatograph (GPC/SEC) with integrated IR5 MCT detector for polyolefin analysis: a breakthrough in sensitivity and automation. In: The applications book, July 2012. LCGC Europe, Chester
43. Ortín A, Montesinos J, López E, del Hierro P, Monrabal B, Torres-Lapasió J, García-Álvarez-Coque MC (2013) Characterization of chemical composition across molar mass distribution in polyolefin copolymers by GPC-IR using a filter-based IR detector. In: Proceedings of the 4th international conference on polyolefin characterization, Houston, October 2012 *Macromolecular Symposia* (in press)
44. Ortín A, López E, Monrabal B, Torres-Lapasió JR, García-Álvarez-Coque MC (2012) *J Chromatogr A* 1257:66–73
45. Wheeler LM, Willis JN (1993) *Appl Spectrosc* 47:1128–1130
46. Willis JN, Dwyer JL, Wheeler LM (1993) *Polym Mater Sci* 69:120–121
47. Verdurmen-Noel L, Baldo L, Bremmers S (2001) *Polymer* 42:5523–5529
48. Kearney T, Dwyer JL (2008) *Am Lab* 40:8–9
49. Carson WW, Dwyer JL, Boumajny B (2008) Copolymer compositional drift across molecular weight measured by LC-FTIR. *Int J Polym Anal* 13:463–470

50. Hiller W, Pasch H, Macko T, Hoffmann M, Ganz J, Spraul M, Braumann U, Streck R, Mason J, Van Damme F (2006) *J Magn Reson* 183:290–302
51. Miller ME, Giddings JC (1998) *J Micro Sep* 10:75–78
52. Mes EPC, de Jonge H, Klein T, Welz R, Gillespie DT (2007) *J Chromatogr A* 1154:319
53. Otte T, Brull R, Macko T, Klein T, Pasch H (2010) *J Chromatogr A* 1217:722–730
54. Otte T, Pasch H, Macko T, Brull R, Stadler FJ, Kaschta J, Becker F, Buback M (2011) *J Chromatogr A* 1218:4257–4267
55. Kamiya T, Ishikawa N, Kambe S, Ikegami N, Nishibu H, Hattori T (1990) *ANTEC Proc.* 1990 48:871–873
56. Starck P (1996) *Polym Int* 40:111
57. Hosoda S (1988) *Polym J* 20:383
58. Flory PJ (1953) *Principles of polymer chemistry*, Chaps XII and XIII. Cornell University Press, Ithaca
59. Huggins ML, Okamoto H (1967) Chapter A: theoretical considerations. In: Cantow MJ (ed) *Polymer fractionation*. Academic, New York, pp 1–66
60. Flory PJ (1948) *Trans Farad Soc* 51:848
61. Wild L, Ryle T, Knobloch D, Peat IR (1982) *J Polym Sci Polym Phys Ed* 20:441
62. Wild L, Blatz C (1993) In: Chung T (ed) *New advances in polyolefins*. Plenum, New York, pp 147–157
63. Alamo R, Mandelkern L (1989) *Macromolecules* 22:1273
64. Monrabal B (1994) *J Appl Polym Sci* 52:491
65. Alamo RG, Glaser RH, Mandelkern L (1988) *J Polym Sci Polym Phys Ed* 26:2169
66. Neves CJ, Monteiro E, Habert AC (1993) *J Appl Polym Sci* 50:817
67. Soares JBP, Hamielec AE (1995) *Macromol Theory Simul* 4:305
68. Glöckner G (1990) *J Appl Polym Sci Appl Polym Symp* 45:1–24
69. Parikh D, Childress BS, Knight GW (1991) *Structural Characterization of LLDPE by STAF ANTEC Conf Proc* 1543
70. Addison A, Ribeiro M, Deffieux A, Fontanille M (1992) *Polymer* 33(20):4337
71. Müller AJ, Hernández ZH, Arnal ML, Sánchez JJ (1997) Successive self-nucleation/annealing (SSA): a novel technique to study molecular segregation during crystallization. *Polym Bull* 39:465–472
72. Keating MY, McCord EF (1994) *Thermochim Acta* 243:129
73. Müller A, Arnal L (2005) *Prog Polym Sci* 30:559–603
74. Wild L, Ryle T (1977) *Polym Prepr* 18:182
75. Wild L, Ryle T, Knobloch D (1982) *Polym Prepr* 3:133
76. Desreux V, Spiegels ML (1950) *Bull Soc Chim Belg* 59:476
77. Hawkins SW, Smith H (1958) *J Polym Sci* 23:341
78. Shirayama K, Okada T, Kita SI (1965) *J Polym Sci A* 3:907
79. Wild L (1991) *Adv Polym Sci* 98:1–47
80. Monrabal B (1996) In: Hosoda S (ed) *New trends in polyolefin science and technology*. Research Signpost, Trivandrum, p 126
81. Fonseca CA, Harrison IR (1999) In: Pethrick RA (ed) *Modern techniques for polymer characterisation*. Wiley, New York, pp 1–13
82. Soares JBP, Hamielec AE (1995) *Polymer* 36(8):1639
83. Soares JBP, Hamielec AE (1999) In: Pethrick RA (ed) *Modern techniques for polymer characterisation*. Wiley, New York, pp 15–55
84. Monrabal B (2000) Temperature rising elution fractionation and crystallization analysis fractionation. In: Meyers RA (ed) *Encyclopedia of analytical chemistry*. Wiley, Chichester, pp 8074–8094
85. Hazlitt LG (1990) *J Appl Polym Sci Appl Polym Symp* 45:25
86. Monrabal B, Ortin A, Romero L (1999) In: *Proceedings of the 12th International symposium on polymer analysis and characterization (ISPAC)*, La Rochelle, 28 June 1999
87. Monrabal B, Sancho-Tello J, Mayo N, Romero L (2007) *Macromol Symp* 257:71–79

88. Yau W, Gillespies D (2001) *Polymer* 42:8947
89. Monrabal B (2004) Microstructure Characterization of Polyolefins. TREF and CRYSTAF. In: Proceedings of the 17th International symposium on polymer analysis and characterization (ISPAC), Heidelberg, 6–9 June 2004
90. Monrabal B, Romero L, Mayo N, Sancho-Tello J (2009) *Macromol Symp* 282:14–24
91. Iiba K, Kusano Y, Sakata K (2010) Novel approach for determination of precise crystallinity distribution by TREF. In: Proceedings 3rd international conference on polyolefin characterization (ICPC), Shanghai, November 2010
92. Boisson C, Boyron O, Macko T, Cossoul E, Baverel Laetitia, Martigny E (2013) Homogeneous copolymers of ethylene with α -olefins synthesized with metallocene catalysts and their use as standards for TREF calibration. In: Proceedings 4th international conference on polyolefin characterization, Houston, October 2012. *Macromolecular Symposia* (in press)
93. Monrabal B, Blanco J, Nieto J, Soares J (1999) *J Polym Sci* 37:89–93
94. Soares J, Monrabal B, Nieto J, Blanco J (1998) *Macromol Chem* 199:1917–1926
95. Stehling CF (1990) International Patent WO 90/03414
96. Davey CR et al (1994) US Patent 5,322,728
97. Monrabal B (2007) Microstructure characterization of polyolefins. In: Abstracts advances in polyolefins, 23–26 September 2007, Santa Rosa. ACS, Division of Polymer Chemistry, Blacksburg
98. Siriwongsarn E, Anantawaraskul S, Chokputtanawuttlerd N, Alghyamah A, Soares J (2012) *Macromol Chem Phys* 213:1892–1906
99. Monrabal B (1991) Crystallization analysis fractionation. US Patent 5,222,390
100. Anantawaraskul S, Soares J, Jirachathorn P (2007) *Macromol Symp* 257:94–102
101. Monrabal B, del Hierro P (2011) Analytical and bioanalytical chemistry. *Sep Sci Macromol* 399(4):1557–1561
102. Monrabal B (2007) CEF. Patent WO 2007/104804 A2
103. Glöckner G (1992) Gradient HPLC of copolymers and chromatographic cross-fractionation. Springer, Berlin
104. Pasch H, Trathnigg B (1998) HPLC of polymers. Springer, Berlin
105. Macko T, Brull R, Zhu Y, Wang Y (2010) *J Sep Sci* 33:3446–3454
106. Lehtinen A, Paukeri R (1994) *Macromol Chem Phys* 195:1539–1556
107. Macko T, Pasch H, Kazakevich YV, Fadeev AY (2003) *J Chromatogr A* 988:69
108. Heinz LC, Pasch H (2005) *Polymer* 46:12040
109. Albrecht A, Heinz LC, Lilge D, Pasch H (2007) *Macromol Symp* 257:46–55
110. Albrecht A, Brüll R, Macko T, Pasch H (2007) *Macromolecules* 40:5545–5551
111. Dolle V, Albrecht A, Brull R, Macko T (2011) *Macromol Chem Phys* 212:959–970
112. Pasch H, Albrecht A, Brüll R, Macko T, Hiller W (2009) *Macromol Symp* 282:71–80
113. Macko T, Pasch H (2009) *Macromolecules* 42:6063–6067
114. Macko T, Brüll R, Wang Y, Coto B, Suarez I (2011) *J Appl Polym Sci* 122:3211–3217
115. Macko T, Brüll R, Alamo RG, Stadler FJ, Losi S (2011) *Anal Bioanal Chem* 399:1547–1556
116. Miller MD, de Groot W, Lyons JW, Van Damme FA, Winniford BL (2012) *J Appl Polym Sci* 123:1238–1244
117. Roy A, Miller MD, Meunier DM, de Groot AW, Winniford WL, Van Damme FA, Pell RJ, Lyons JW (2010) *Macromolecules* 43:3710–3720
118. Ginsburg A, Macko T, Dolle V, Bruell R (2011) *Eur Polym J* 47:319–329
119. Cheruthazhekatt S, Pijpers TFJ, Harding GW, Mathot VBF, Pasch H (2012) *Macromolecules* 45:2025–2034
120. Chang T, Lee HC, Lee W, Park S, Ko C (1999) *Macromol Chem Phys* 200(10):2188
121. Cong R, de Groot AW, Parrott A, Yau W, Hazlitt L, Brown R, Cheatham M, Miller MD, Zhou Z (2012) *Macromol Symp* 312:108–114
122. Cong R, de Groot W, Parrott A, Yau W, Hazlitt L, Brown R, Miller M, Zhou Z (2011) *Macromolecules* 44:3062–3072
123. Monrabal B, Mayo N, Cong R (2012) *Macromol Symp* 312:115–129
124. Cong et al (2011) Patent WO 084786 A1

125. Cong et al (2012) Determination of the microstructure of polyolefins using thermal gradient interaction chromatography and its hyphenated techniques. In: Proceedings 4th international conference on polyolefin characterization, Houston, October 2012
126. Monrabal B (2011) New tools in the characterization of polyolefin microstructure. In: Abstracts advances in polyolefins, 25–28 September 2011, Santa Rosa. ACS, Polymer Chemistry Division, Blacksburg
127. Monrabal B, Lopez E (2013) Advances in thermal gradient interaction chromatography and crystallization techniques for composition analysis in polyolefins. In: Proceedings of the 4th international conference on polyolefin characterization, Houston, October 2012. Macromolecular symposia 2013 (in press)
128. Aust N, Beytollahi-amtmann I, Lederer K (1995) *Int J Polym Anal Character* 1:245
129. Faldi A, Soares JBP (2001) *Polymer* 42:3057–3066
130. Nakano, Goto Y (1981) Mitsubishi Petrochemical Co, Ltd. *J Appl Polym Sci* 26:4217–4231
131. Li Pi Shan C, Gillespie D, Hazlitt L (2005) The Dow Chemical Company. Ecorep, Lyon
132. Gillespie D, Hazlitt L, Li Pi Shan C (2006) In: Proceedings 1st international conference on polyolefin characterization (ICPC), Houston, October 2006
133. Ortín A, Monrabal B, Sancho-Tello J (2007) *Macromol Symp* 257:13–28
134. Monrabal B (2012) Advances in microstructure characterization of polyolefins. In: Proceedings Chemelot International Polyolefins Symposium (CIPS), Maastricht, 7–10 October 2012